Supporting Information For

Observation-constrained projection of flood risks and socioeconomic exposure in China

Shengyu Kang[a], Jiabo Yin[a*], Lei Gu[a*], Yuanhang Yang[a], Dedi Liu[a], Louise Slater[b]

[a] State Key Laboratory of Water Resources Engineering and Management, Wuhan University, Wuhan, Hubei, 430072, P.R. China

[b] School of Geography and the Environment, University of Oxford, Oxford, UK

*Correspondence: J. Yin (jboyn@whu.edu.cn); L. Gu (shisan@whu.edu.cn)

Contents of this file

Table S1: List of the 5 selected GCMs from CMIP6

ID	GCM Name	Institute	Horizontal resolution (lon. × lat.)
1	IPSL-CM6A-LR	Institut Pierre Simon Laplace	2.50° × 1.27°
2	GFDL-ESM4	Geophysical Fluid Dynamics Laboratory	1.25° × 1°
3	MPI-ESM1-2-HR	Max Planck Institute for Meteorology	0.9° × 0.9°
4	MRI-ESM2-0	Meteorological Research Institute	1.125° × 1.125°
5	UKESM1-0-LL	Natural Environment Research Council and Met office	1.25° × 1.875°

Table S2: Various components and the related mechanics of the model.

Components/Mechanics	Variables/Parameters	Description	Strength and weaknesses
In situ streamflow over 463 catchments	Daily streamflow (R_{obs})	Inputs of four HMs	This dataset is a comprehensive daily streamflow dataset for China, but contains data gaps.
Gridded meteorological dataset in China	*pr*, daily max/min T_{2m}	Inputs of four HMs	This dataset is derived from official agencies, but contains a limited number of variables.
ERA5-Land	*pr, ps, SH, RH, rlds, rsds,* T_{2m}	Processed as daily scale	The dataset contains many variables with a high spatiotemporal resolution, but it is reanalysis data, i.e. not observations.
ISIMIP3b	Same as ERA5-Land	Drive HM-LSTM models for future streamflow simulation	Bias-corrected CMIP6 data are provided, but few GCMs are available.
HM	GR4J, HBV, HMETS, XAJ	Output streamflow (R_{HM})	HMs can capture physical hydrological processes well, but it cannot characterize human activity impacts.
Lag time	*pr, ps, SH, RH, rlds, rsds,* T_{2m}, R_{HM}	Prepare inputs for the LSTM layer	Adding available variables for LSTM, but it exponentially increases the consumption of computational resources.
LSTM	64 hidden units and a fully connected layer	Optimize and correct R_{HM} using the above inputs	A machine learning approach is introduced, but physical mechanisms need to be explored.

Text S1 The screening process of selecting catchments

We collected daily streamflow data from 1961 to 2016 at outlets of 463 catchments over China (Figure S1a), and a strict data quality control was carried out to select catchments following three procedures.

(1) Measurement errors and inconsistencies (e.g., changing instruments or station datum) were identified, and only those stations with more than 20 valid years of data (>90% completeness from April to October) were retained.

(2) Catchments with overlapping areas were identified, and we chose to remove the catchments with the largest area. As the inputs in our conceptual lumped hydrological models are basin average meteorological series, the catchments with large areas are less able to represent the spatial heterogeneity of meteorological variations. For example, it is challenging to perform hydrological simulation in the control basin of Yichang station (with catchment area of about 1 million km2). After omitting the overlapping catchments, we retained 215 basins.

(3) Only catchments where at least one model had satisfactory performance (KGE > 0.55 in daily streamflow simulation) were selected. As our developed HM-LSTM model can improve simulation skills, only 11 catchments with poor performance were eliminated.

The selected 204 catchments cover the eight major river basins in China except for the Northwest River basin (Figure S1b). The absence of this part of the catchment does not affect our study because the high mountains hinder the atmospheric moisture transport to northwestern China, so that floods rarely occur there (Yin et al., 2021). To

date, conducting hydrological simulation in a large sample of catchments in China is still a challenging issue due to lack of data. Numerous studies have only focused on a smaller number of catchments in China. For example, Yin et al. (2021) evaluated the shifts in flood risk in 151 catchments, which showed great advances in assessing large-scale flood risks over China.

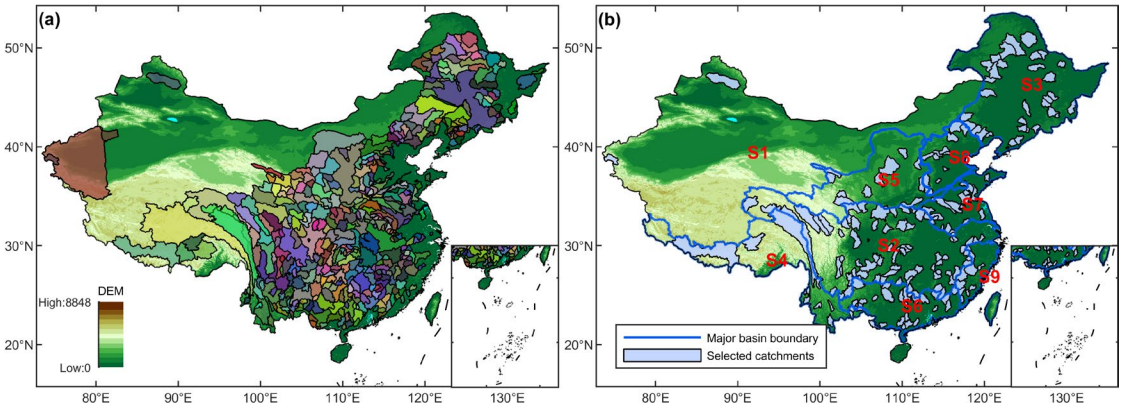

Figure S1. Distribution of studied catchments over mainland China. (a) The distribution of all 463 catchments. (b) The selected 204 catchments and nine major river basins (S1-Northwest River basins, S2-Yangtze River basin, S3-Songliao River basins, S4-Southwest River basins, S5-Yellow River basin, S6-Zhu River basin, S7-Huaihe River basin, S8-Haihe River basin, S9-Southeast River basins).

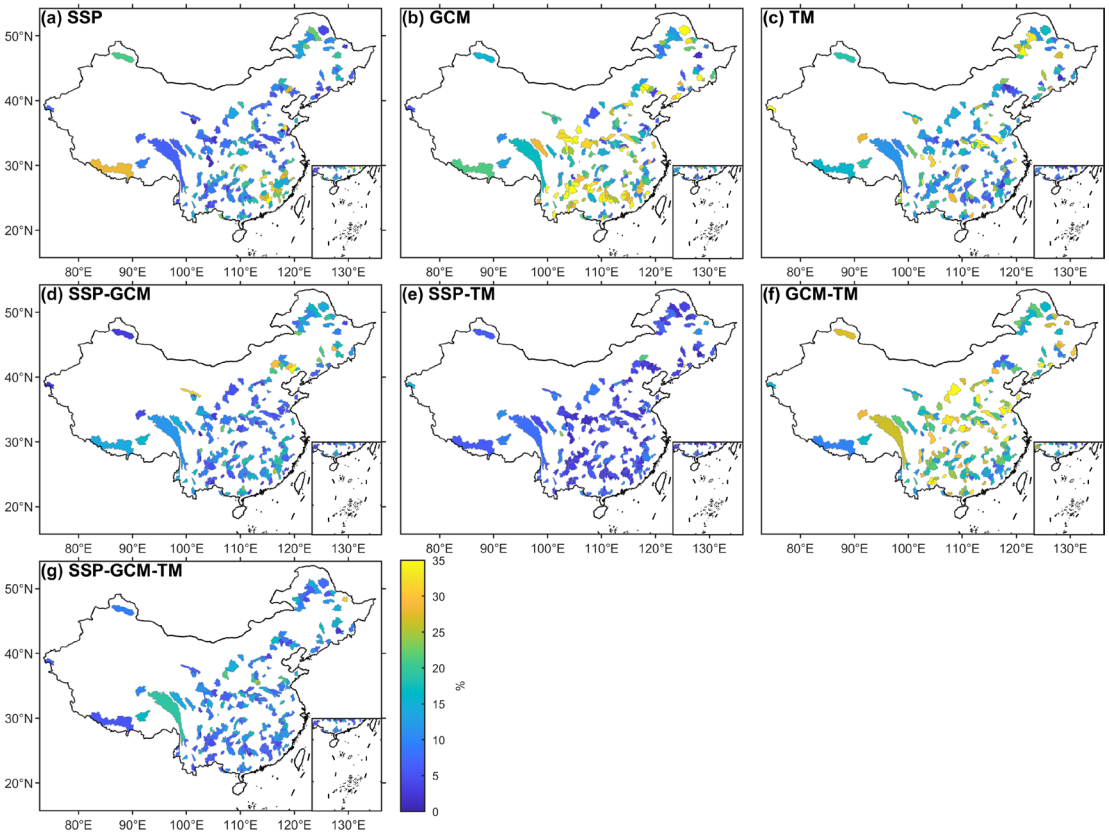

Figure S2. Uncertainty decomposition of GDP in selected 204 catchments. a-g, Uncertainty contribution sourced from SSP (a), GCM (b), TM (c), SSP-GCM (d), SSP-TM (e), GCM-TM (f), SSP-GCM-TM (g).

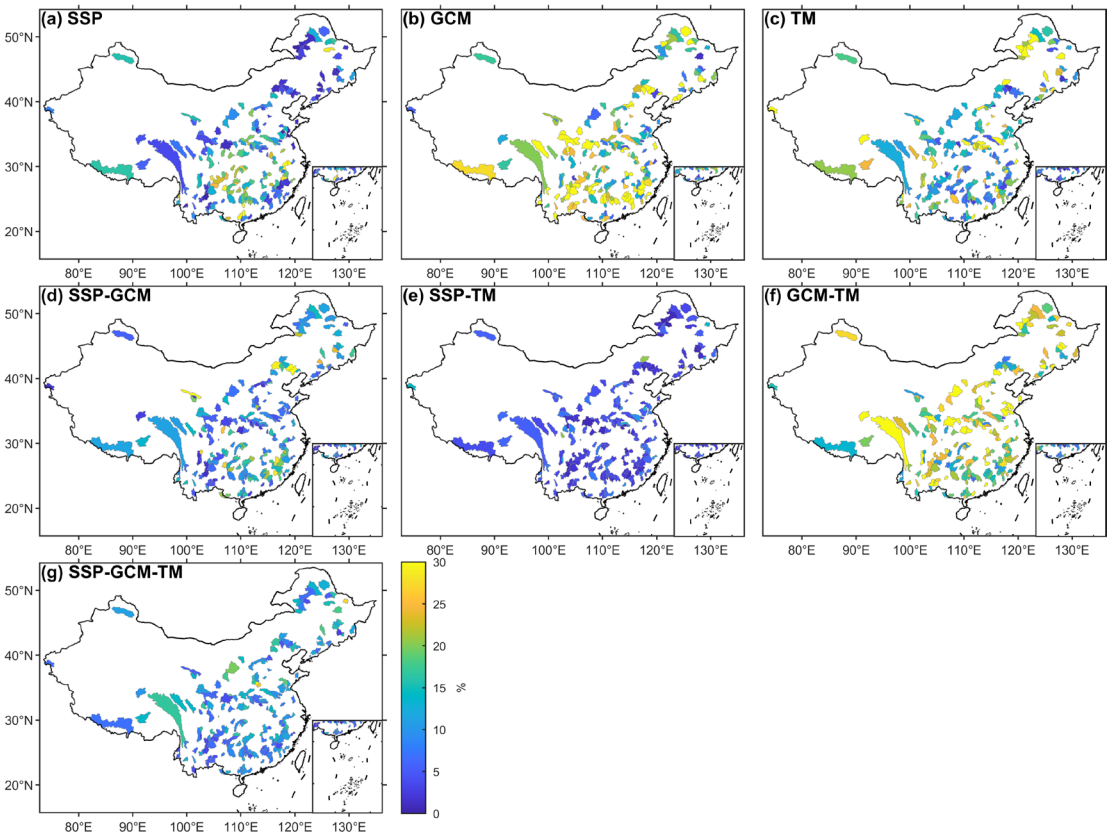

Figure S3. Uncertainty decomposition of population in selected 204 catchments. a-g, Uncertainty contribution sourced from SSP (a), GCM (b), TM (c), SSP-GCM (d), SSP-TM (e), GCM-TM (f), SSP-GCM-TM (g).

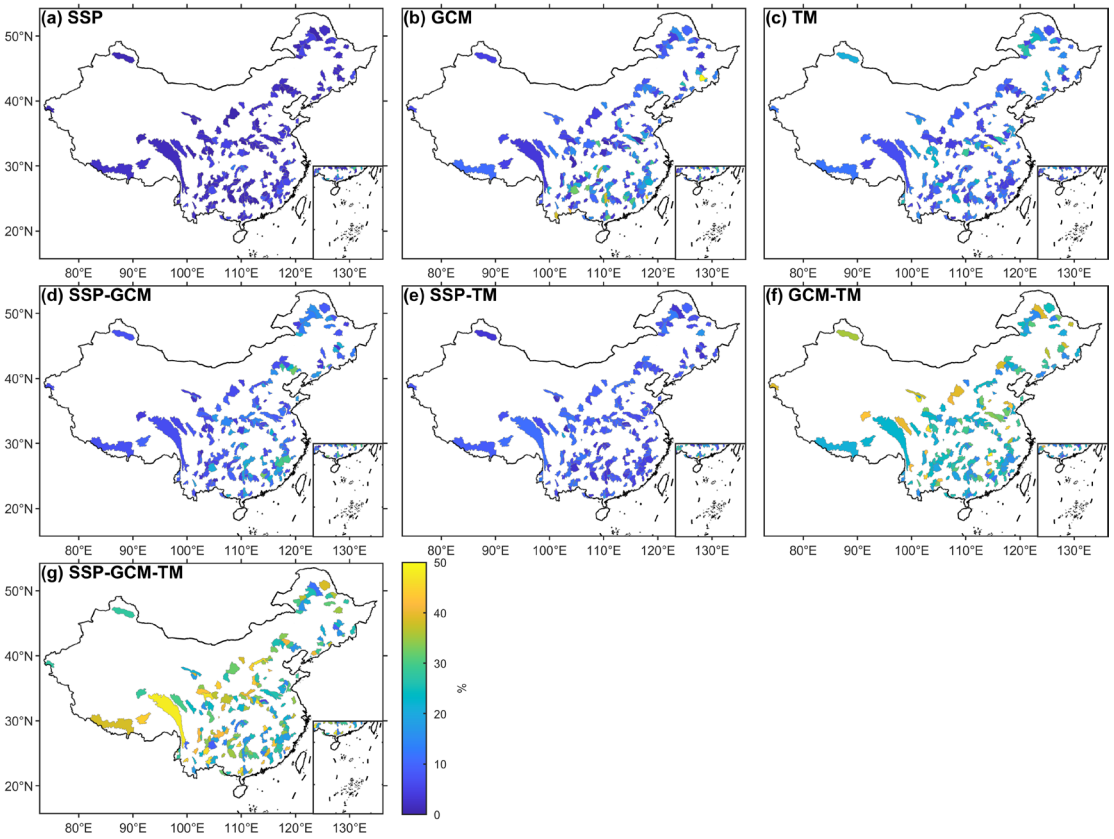

Figure S4. Uncertainty decomposition of JRP in selected 204 catchments. a-g, Uncertainty contribution sourced from SSP (a), GCM (b), TM (c), SSP-GCM (d), SSP-TM (e), GCM-TM (f), SSP-GCM-TM (g).

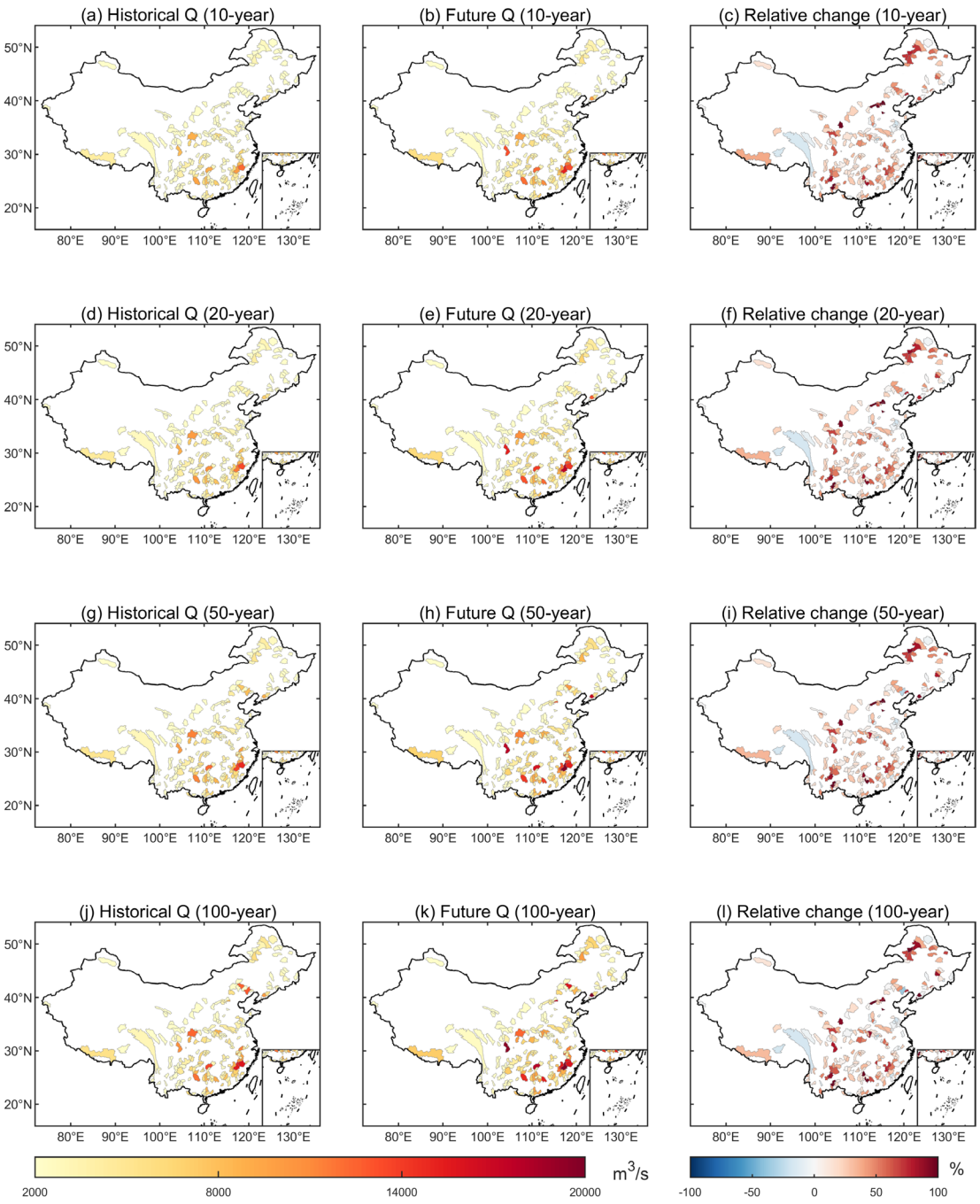

Figure S5. Design flood peaks under four RPs and relative change from historical to future periods. The daily streamflow series are projected by using outputs of UKESM1-0-LL under SSP1-26.

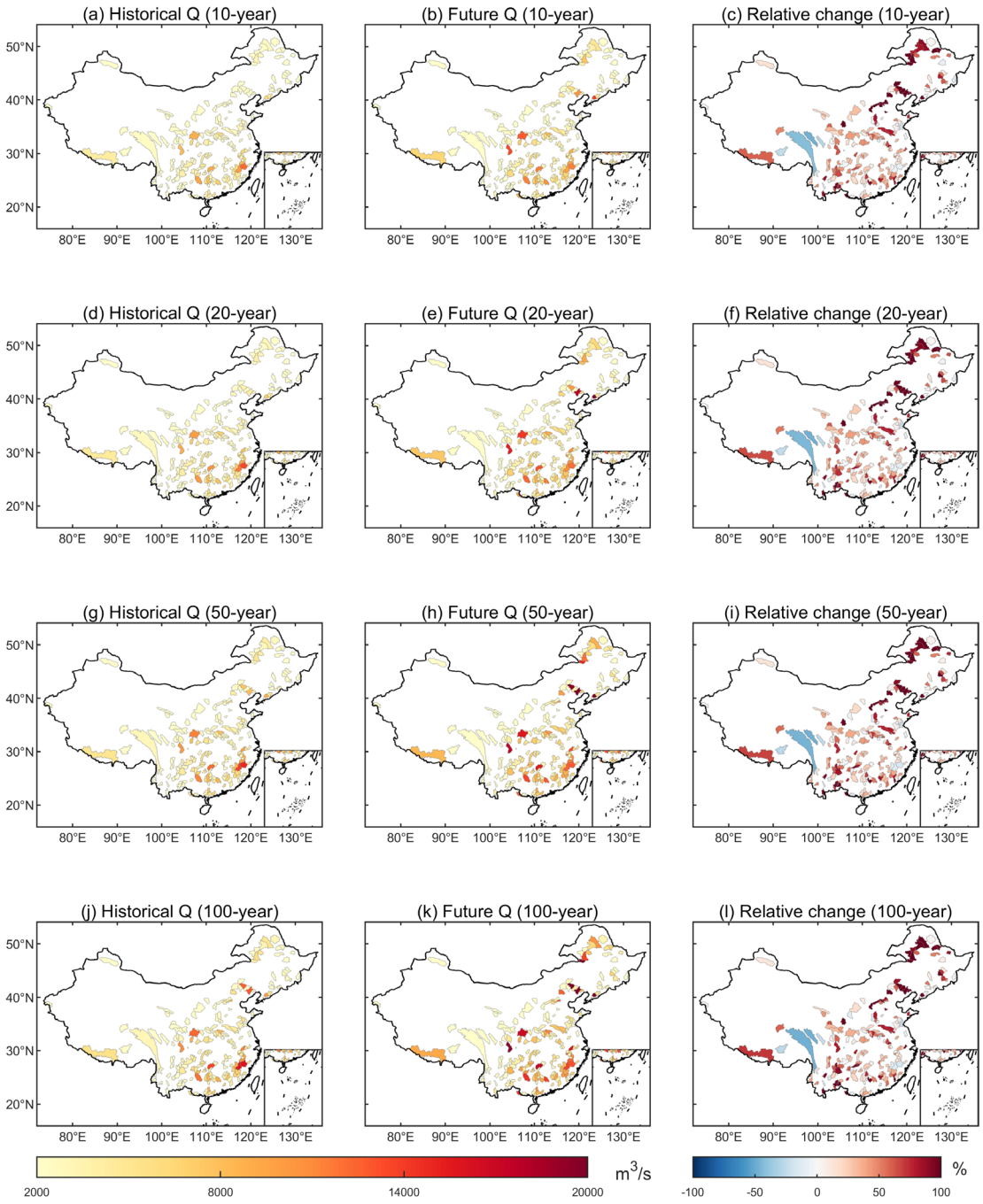

Figure S6. Design flood peaks under four RPs and relative change from historical to future periods. The daily streamflow series are projected by using outputs of UKESM1-0-LL under SSP3-70.

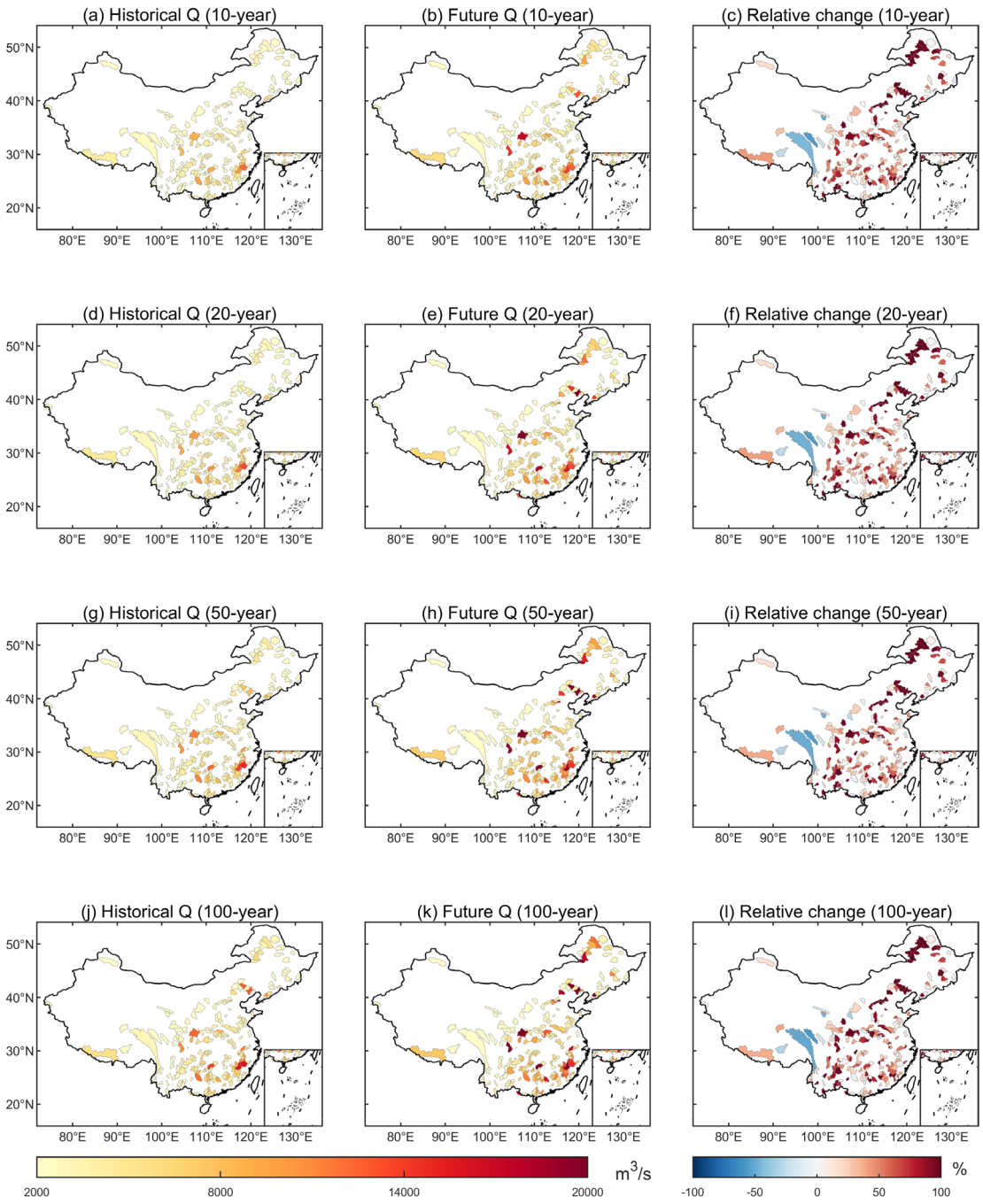

Figure S7. Design flood peaks under four RPs and relative change from historical to future periods. The daily streamflow series are projected by using outputs of UKESM1-0-LL under SSP5-85.

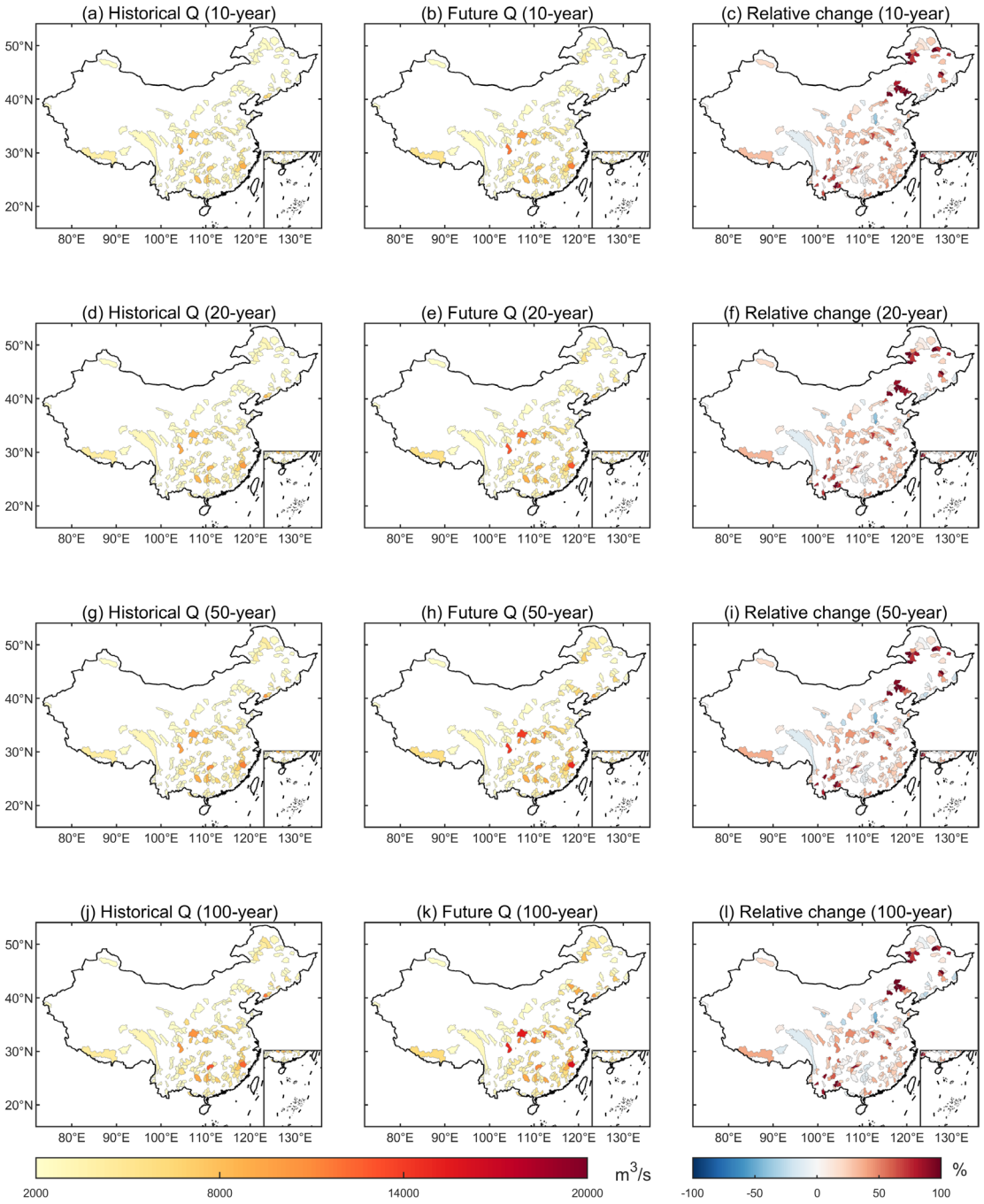

Figure S8. Design flood peaks under four RPs and relative change from historical to future periods. The daily streamflow series are projected by using outputs of MRI-ESM2-0 under SSP1-26.

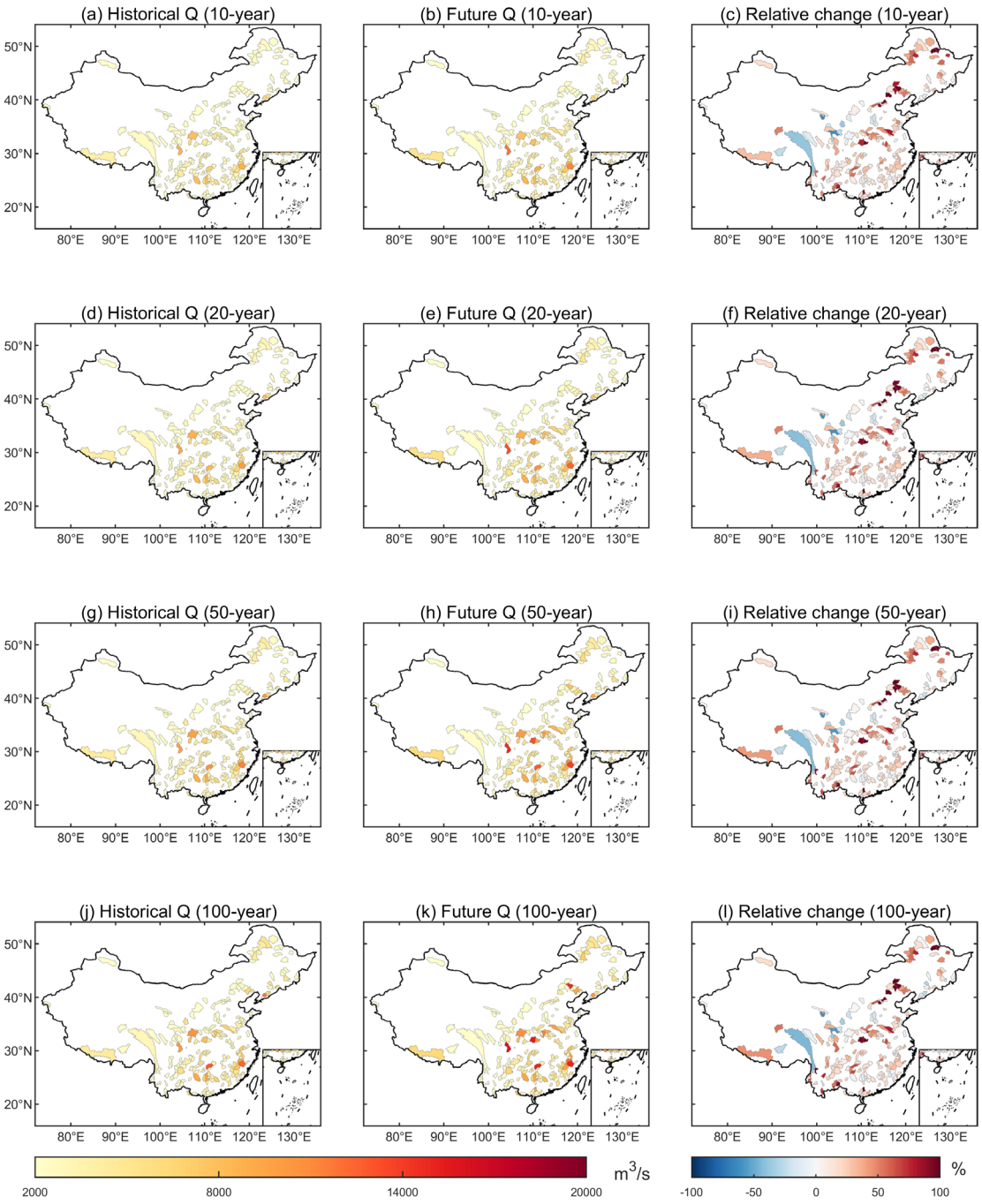

Figure S9. Design flood peaks under four RPs and relative change from historical to future periods. The daily streamflow series are projected by using outputs of MRI-ESM2-0 under SSP3-70.

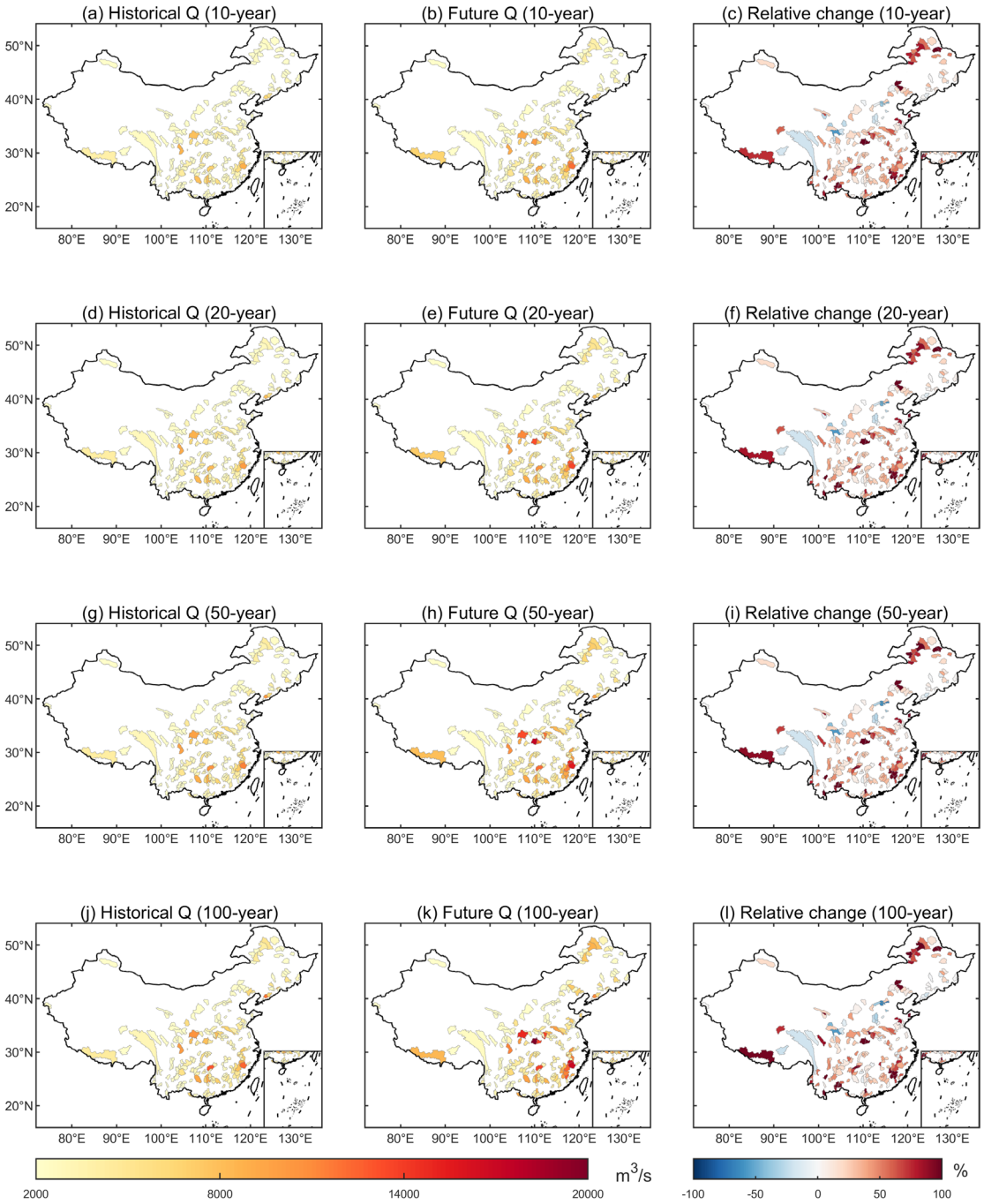

Figure S10. Design flood peaks under four RPs and relative change from historical to future periods. The daily streamflow series are projected by using outputs of MRI-ESM2-0 under SSP5-85.

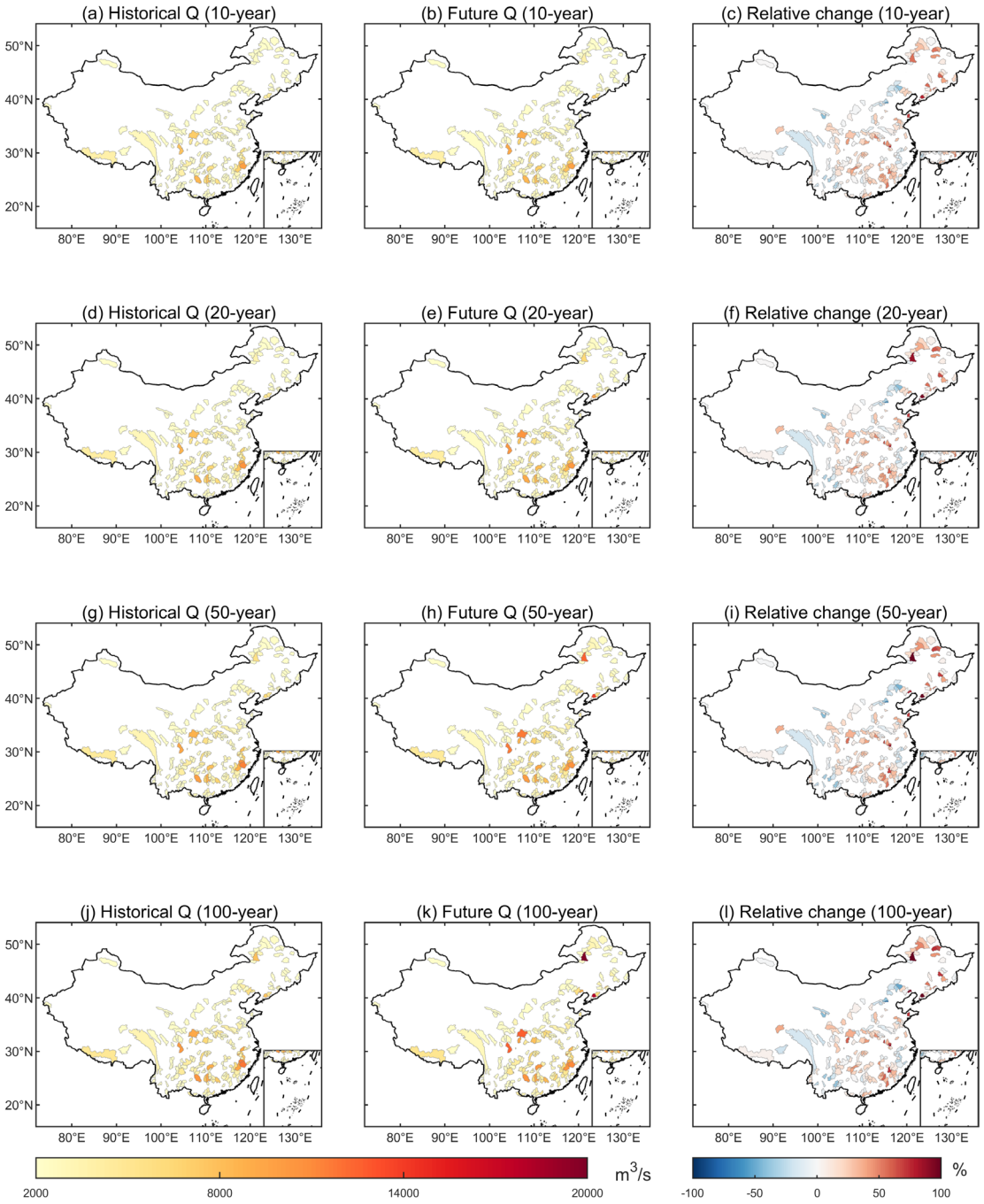

Figure S11. Design flood peaks under four RPs and relative change from historical to future periods. The daily streamflow series are projected by using outputs of MPI-ESM1-2-HR under SSP1-26.

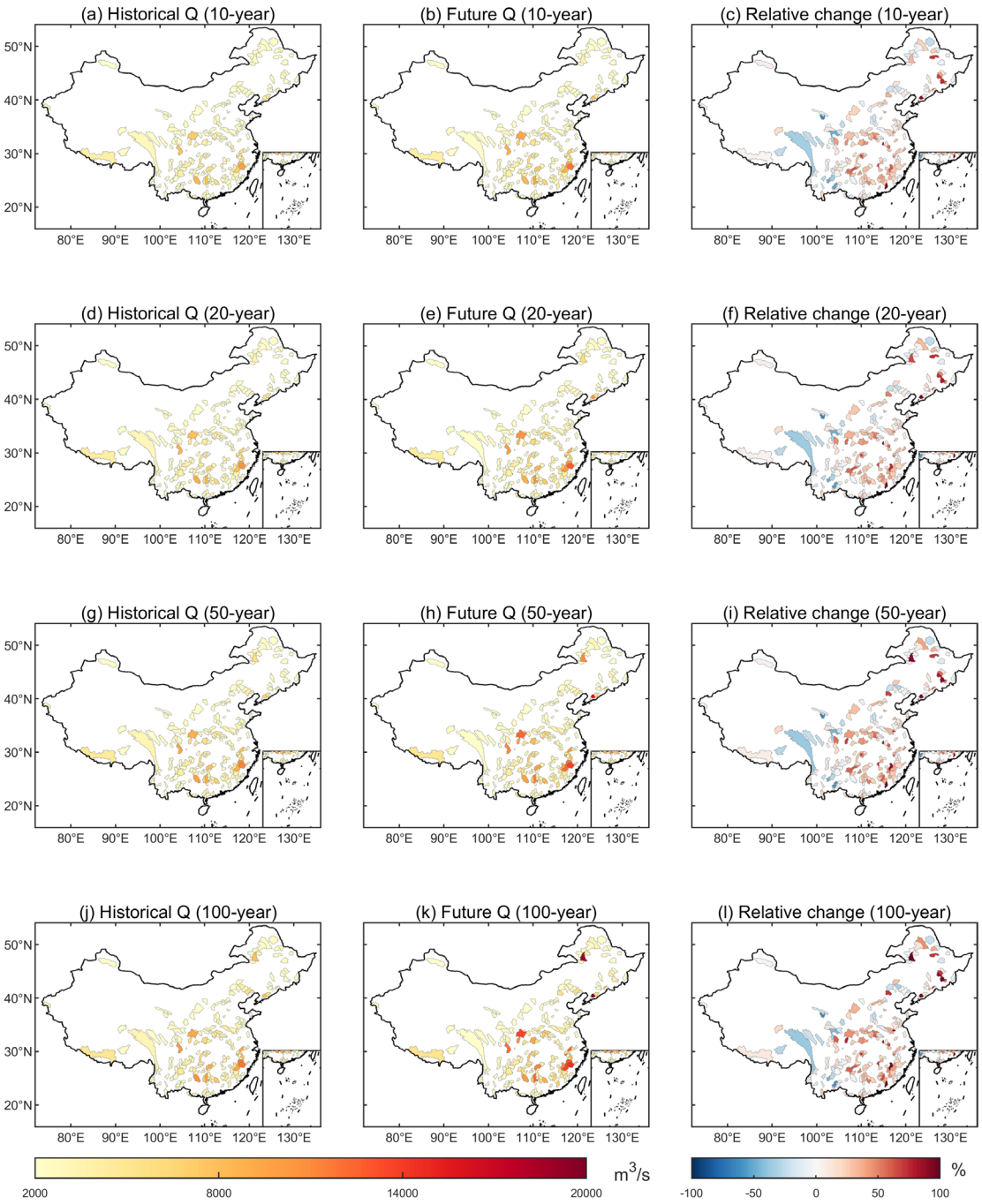

Figure S12. Design flood peaks under four RPs and relative change from historical to future periods. The daily streamflow series are projected by using outputs of MPI-ESM1-2-HR under SSP3-70.

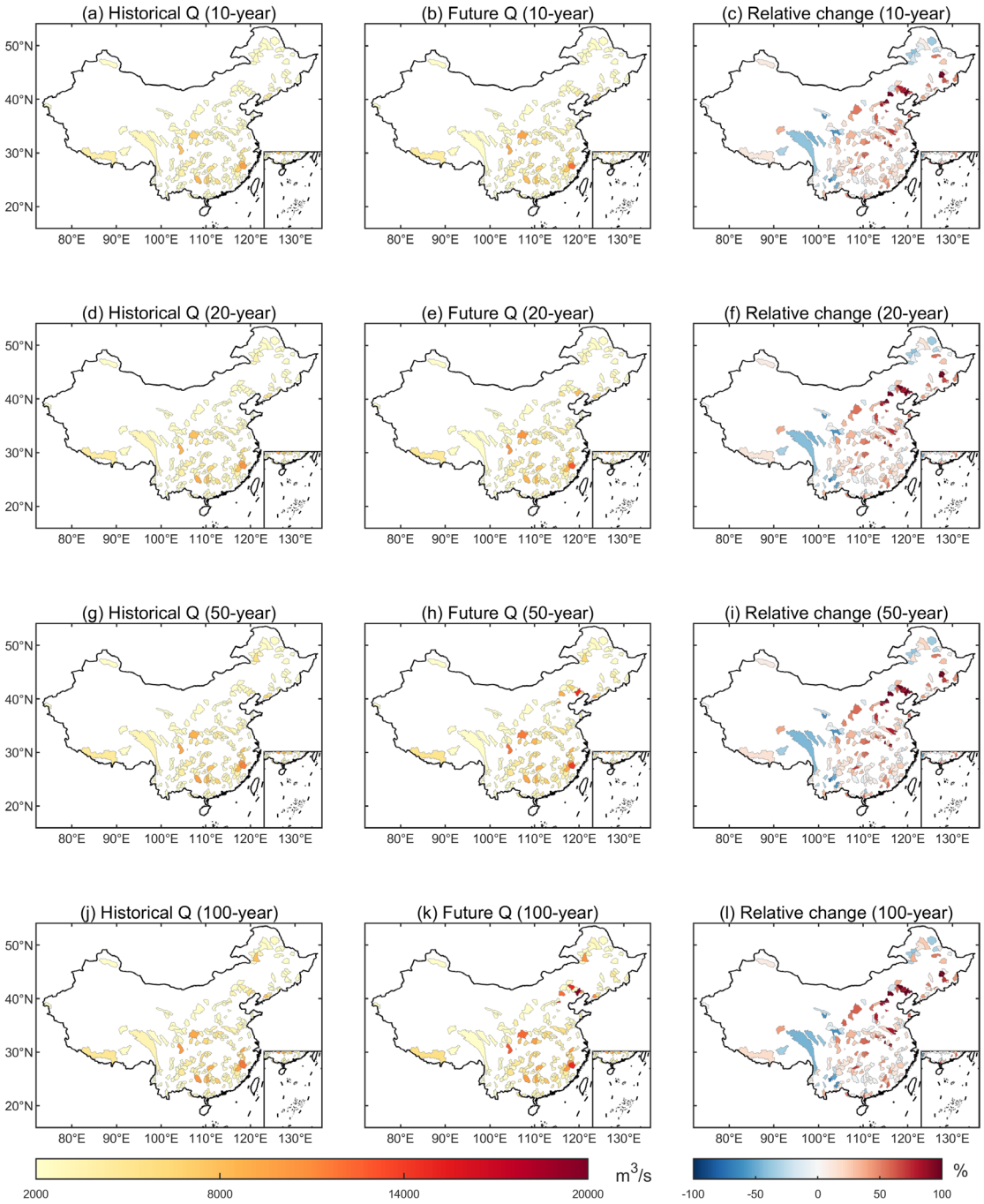

Figure S13. Design flood peaks under four RPs and relative change from historical to future periods. The daily streamflow series are projected by using outputs of MPI-ESM1-2-HR under SSP5-85.

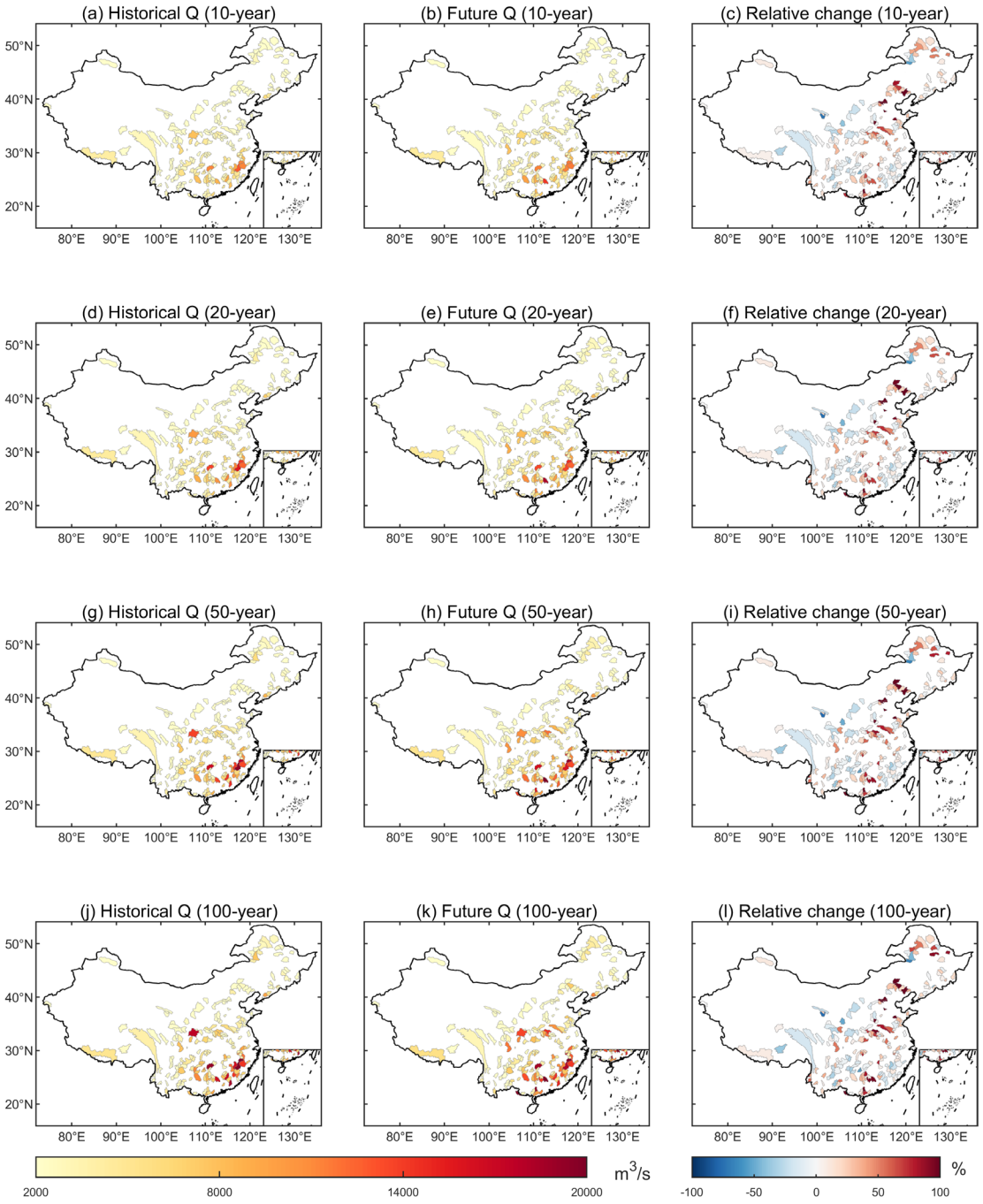

Figure S14. Design flood peaks under four RPs and relative change from historical to future periods. The daily streamflow series are projected by using outputs of IPSL-CM6A-LR under SSP1-26.

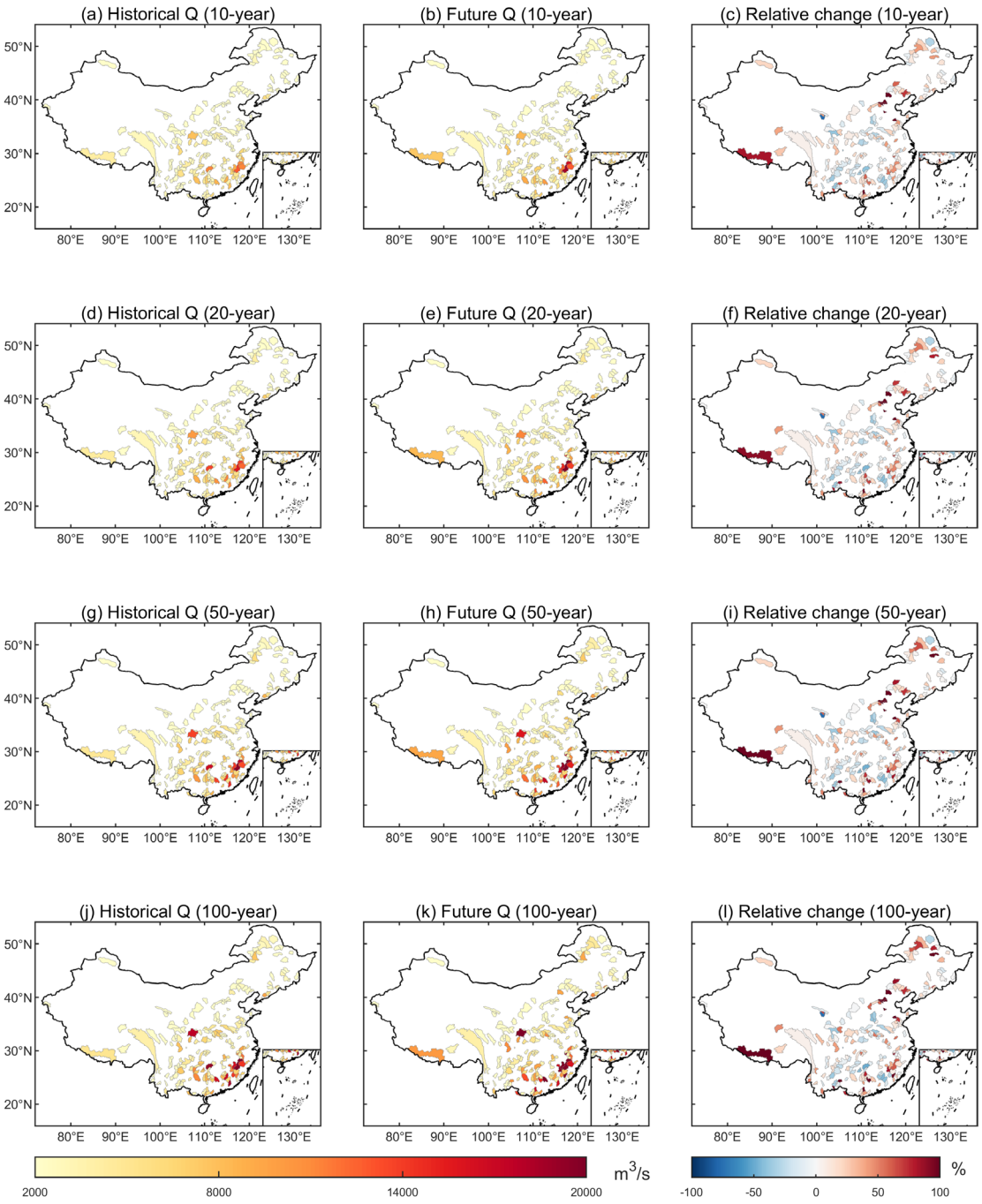

Figure S15. Design flood peaks under four RPs and relative change from historical to future periods. The daily streamflow series are projected by using outputs of IPSL-CM6A-LR under SSP3-70.

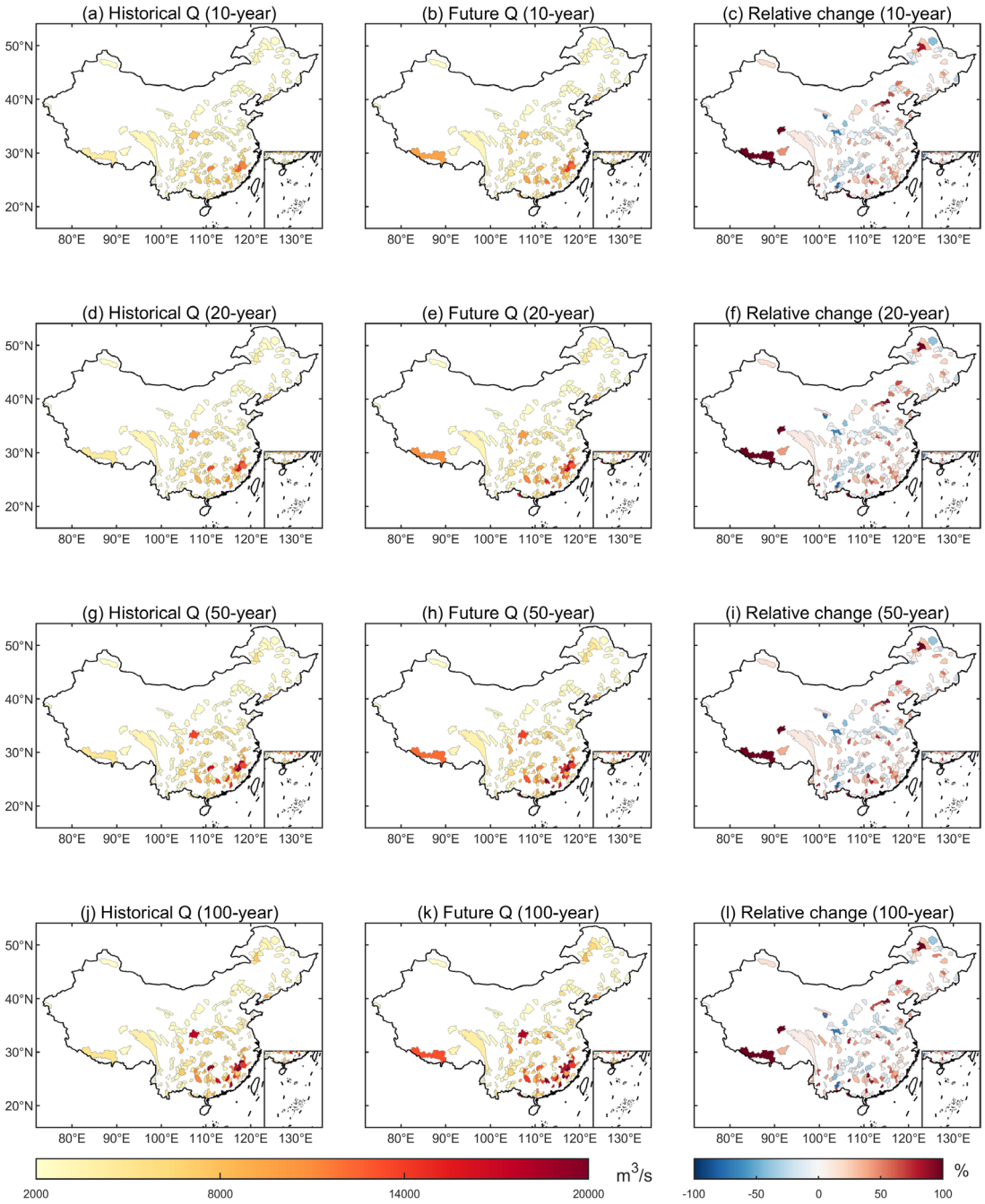

Figure S16. Design flood peaks under four RPs and relative change from historical to future periods. The daily streamflow series are projected by using outputs of IPSL-CM6A-LR under SSP5-85.

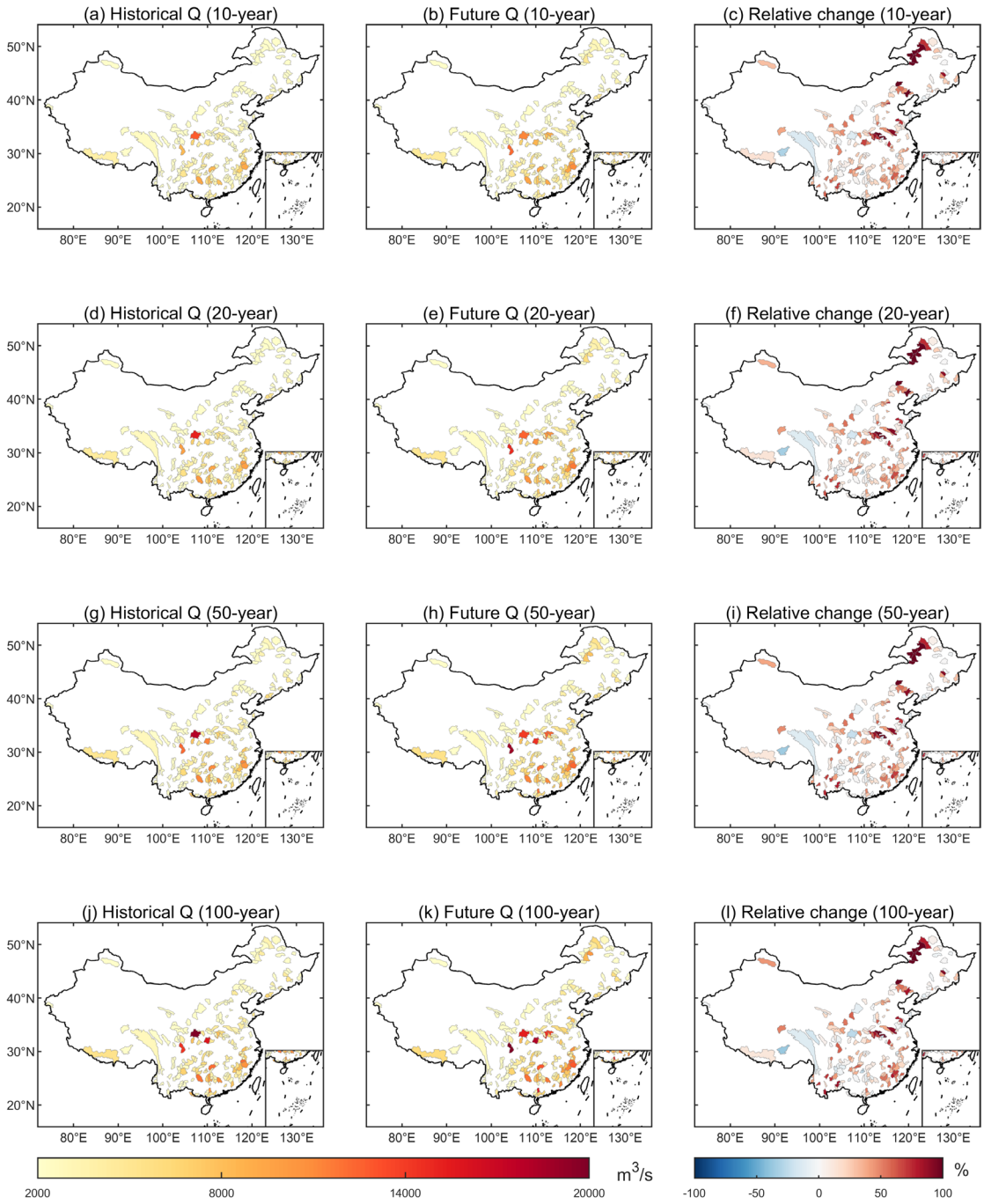

Figure S17. Design flood peaks under four RPs and relative change from historical to future periods. The daily streamflow series are projected by using outputs of GFDL-ESM4 under SSP1-26.

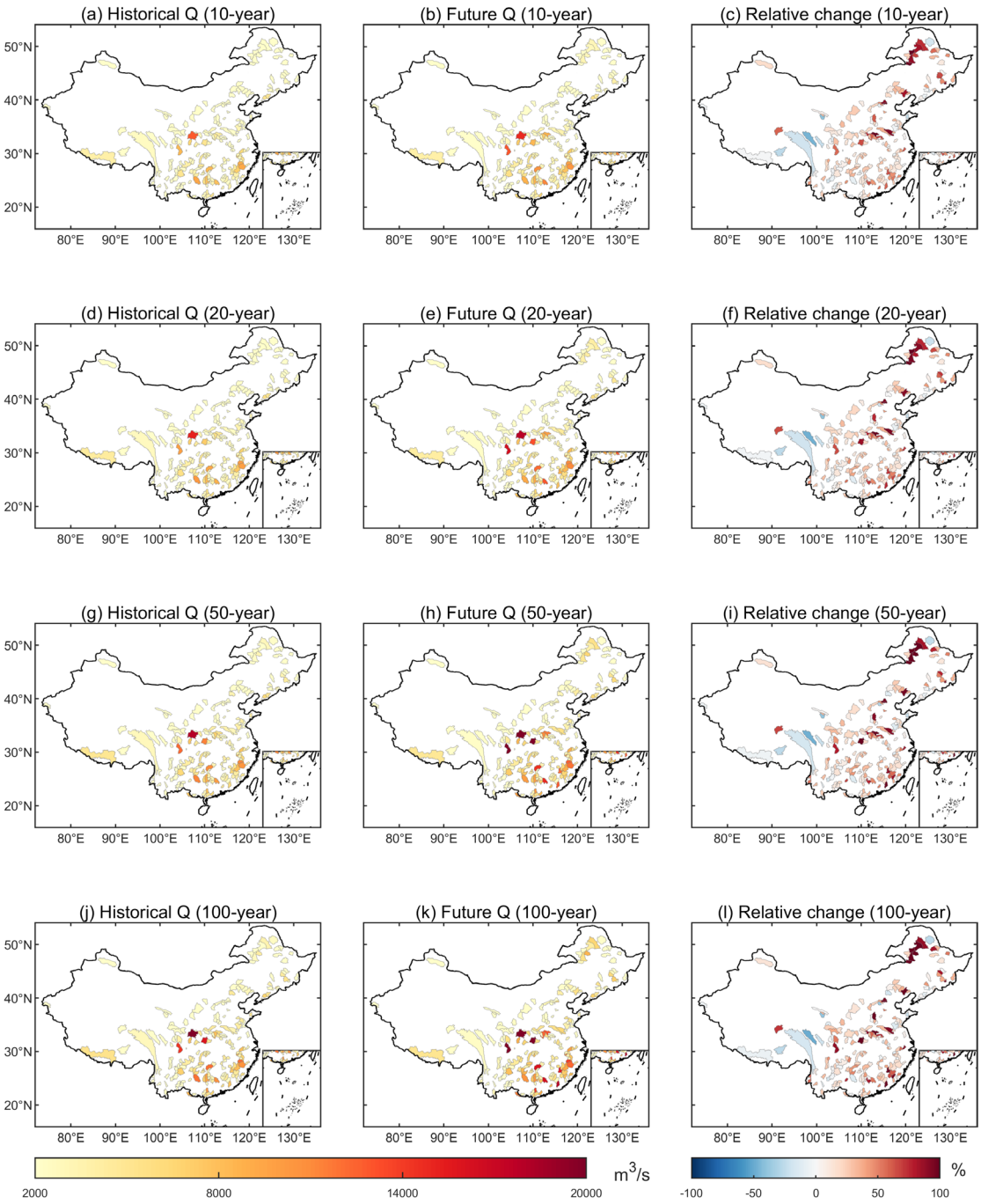

Figure S18. Design flood peaks under four RPs and relative change from historical to future periods. The daily streamflow series are projected by using outputs of GFDL-ESM4 under SSP3-70.

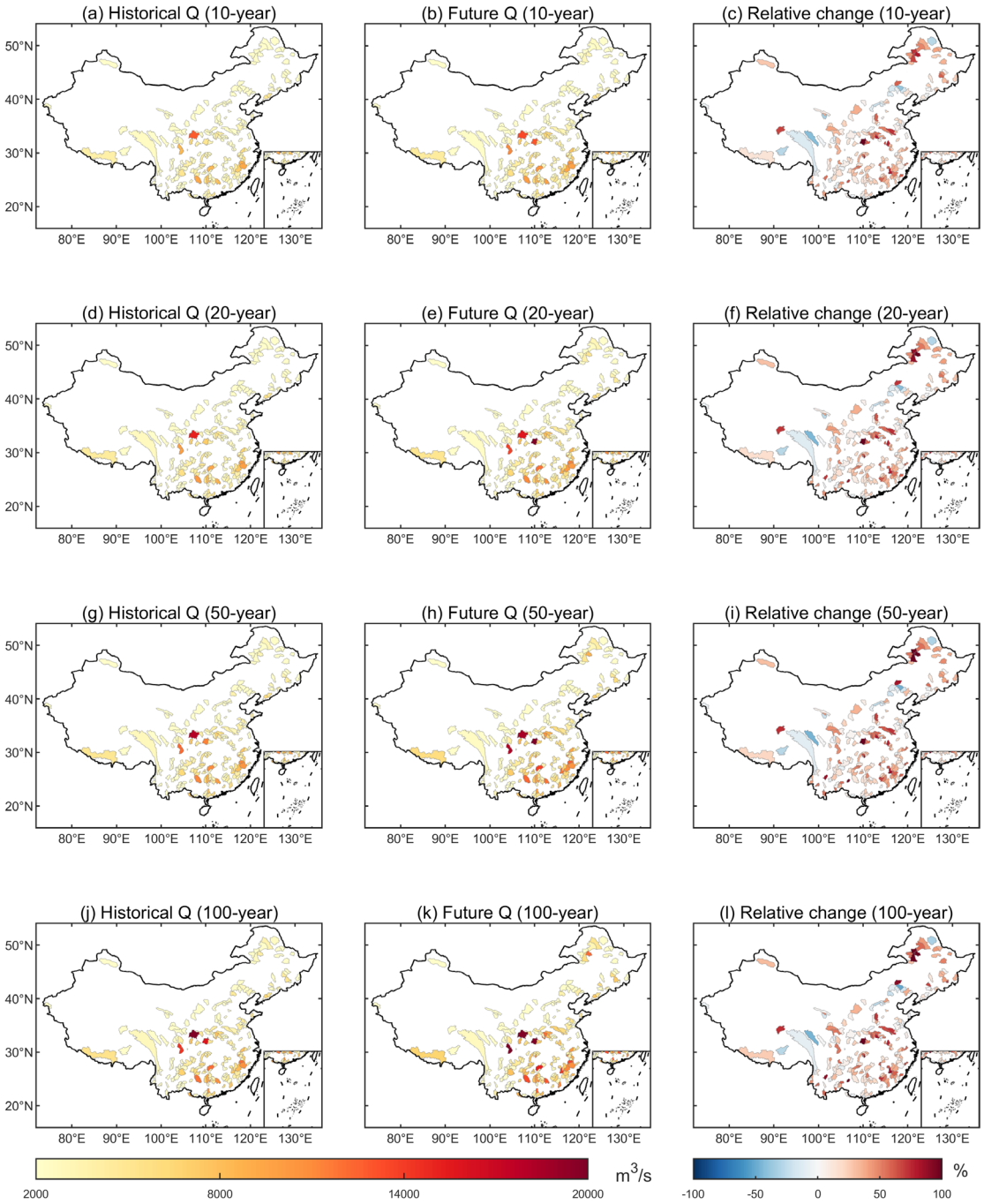

Figure S19. Design flood peaks under four RPs and relative change from historical to future periods. The daily streamflow series are projected by using outputs of GFDL-ESM4 under SSP5-85.

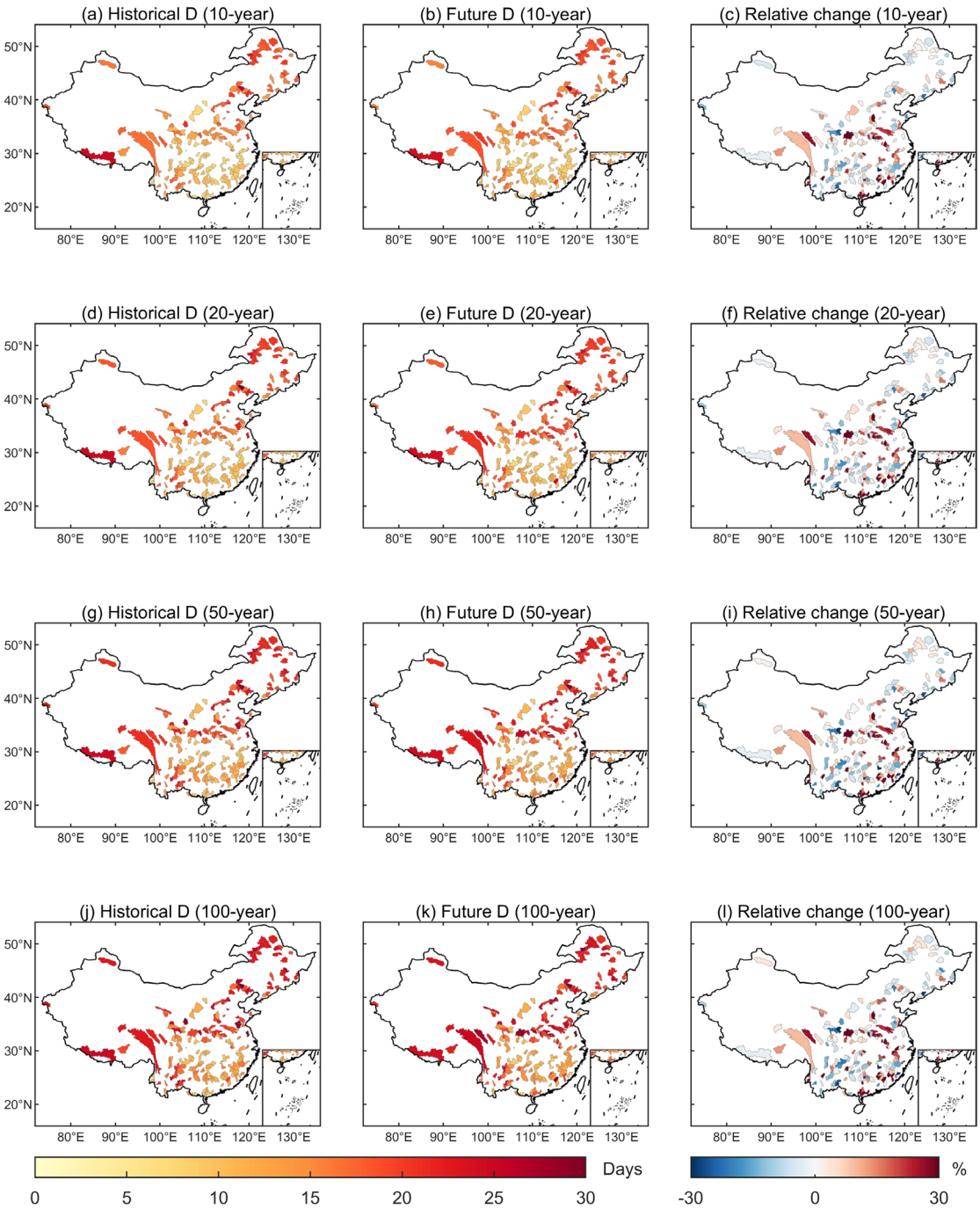

Figure S20. Flood duration under four RPs and relative change from historical to future periods. The daily streamflow series are projected by using outputs of UKESM1-0-LL under SSP1-26.

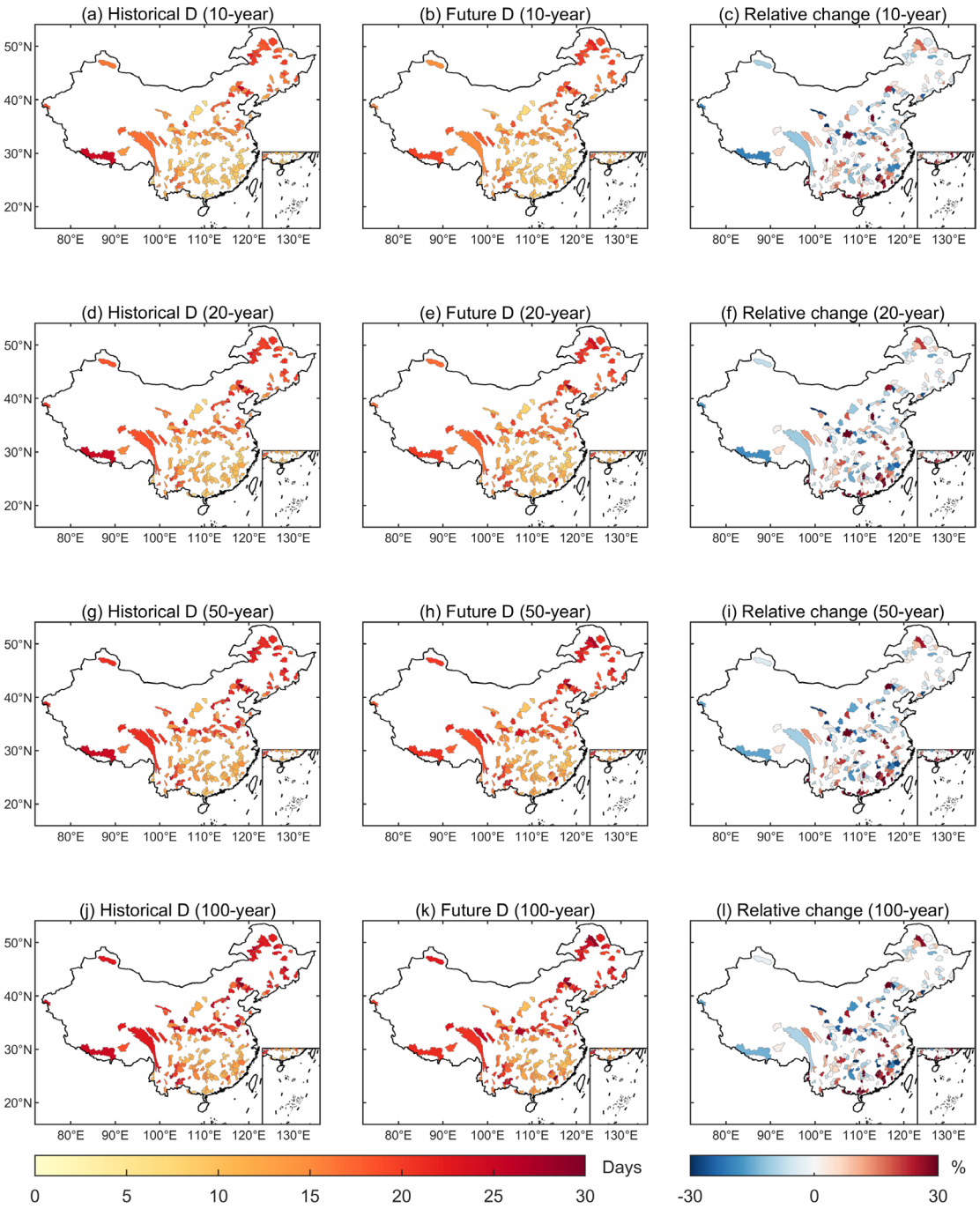

Figure S21. Flood duration under four RPs and relative change from historical to future periods. The daily streamflow series are projected by using outputs of UKESM1-0-LL under SSP3-70.

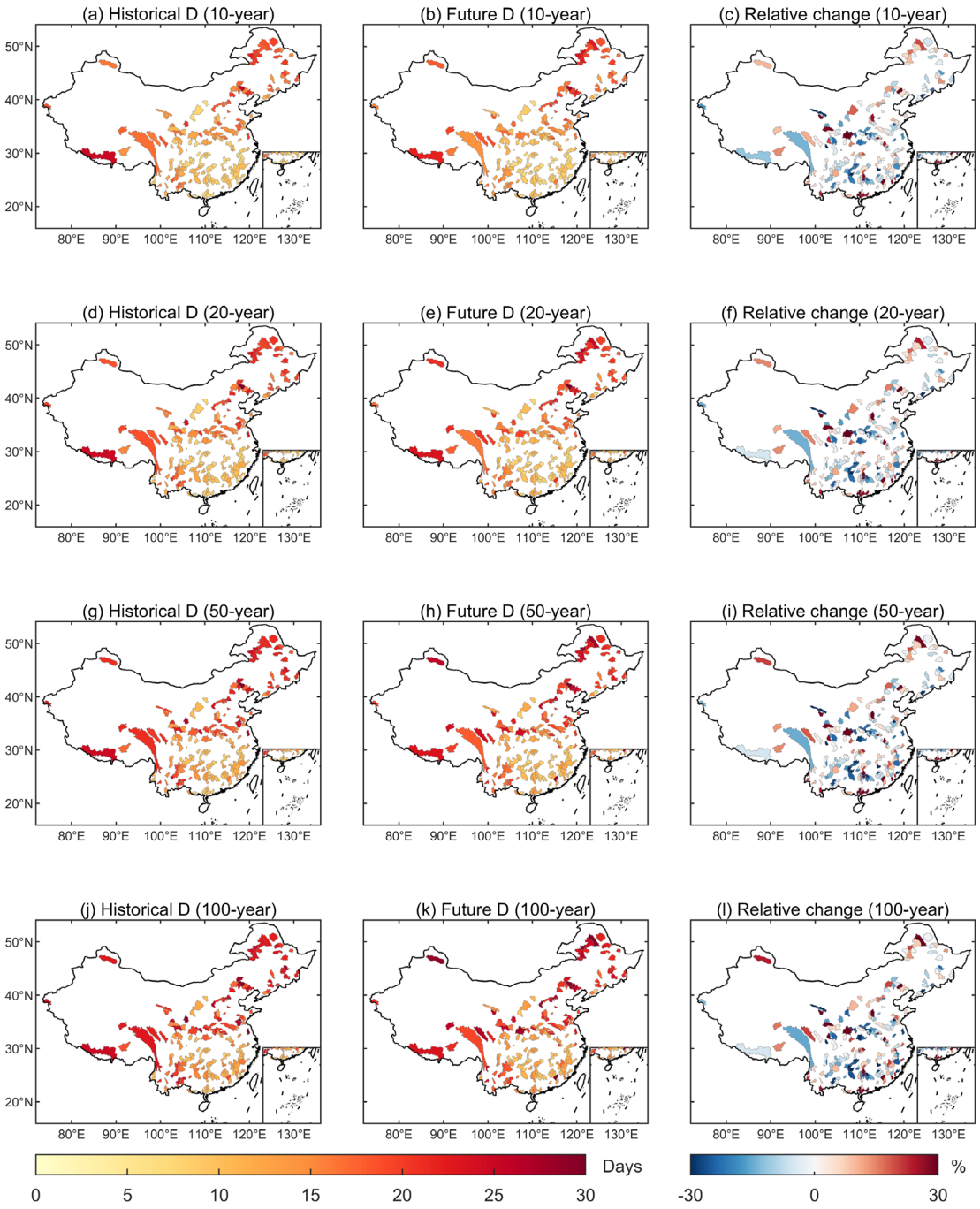

Figure S22. Flood duration under four RPs and relative change from historical to future periods. The daily streamflow series are projected by using outputs of UKESM1-0-LL under SSP5-85.

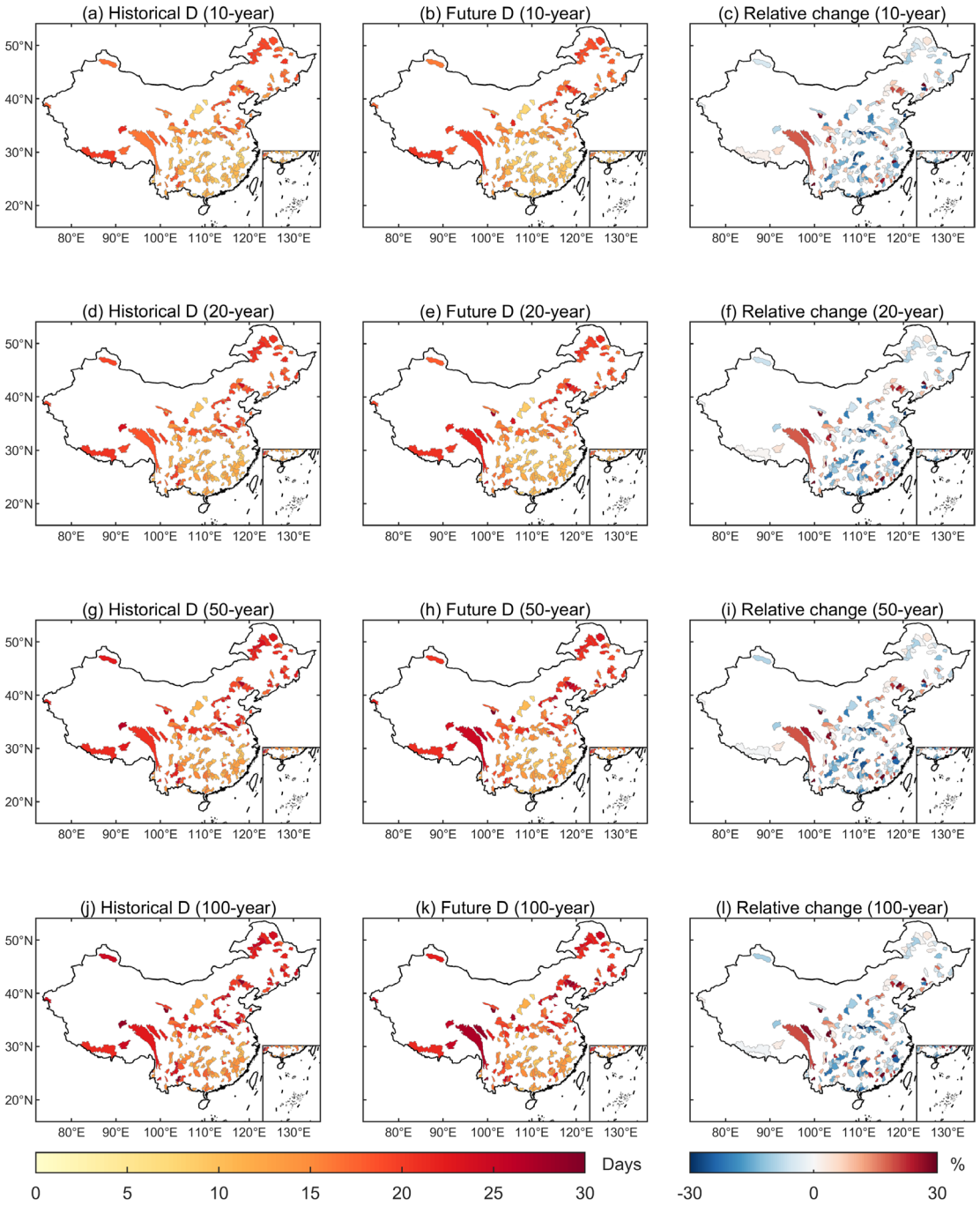

Figure S23. Flood duration under four RPs and relative change from historical to future periods. The daily streamflow series are projected by using outputs of MRI-ESM2-0 under SSP1-26.

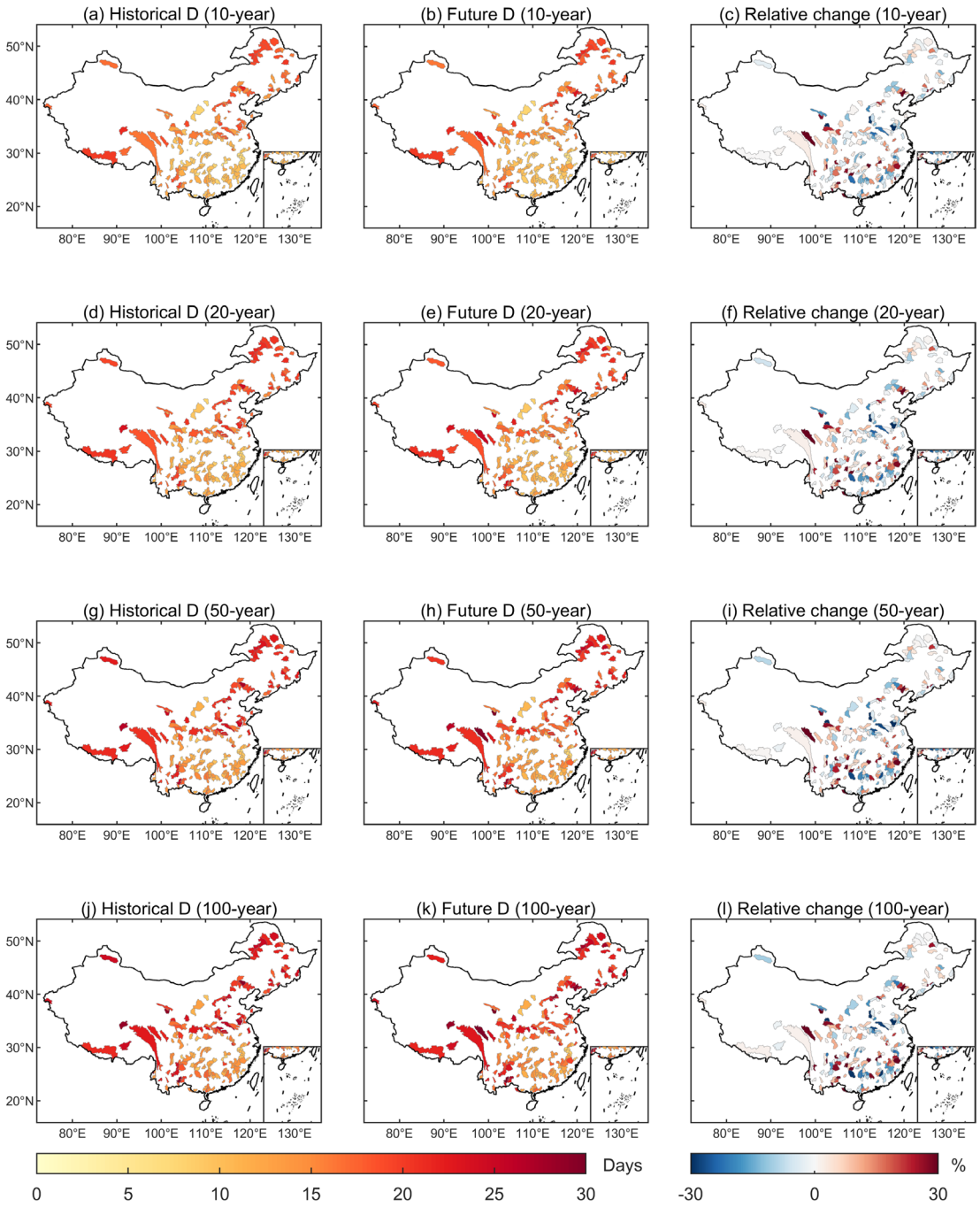

Figure S24. Flood duration under four RPs and relative change from historical to future periods. The daily streamflow series are projected by using outputs of MRI-ESM2-0 under SSP3-70.

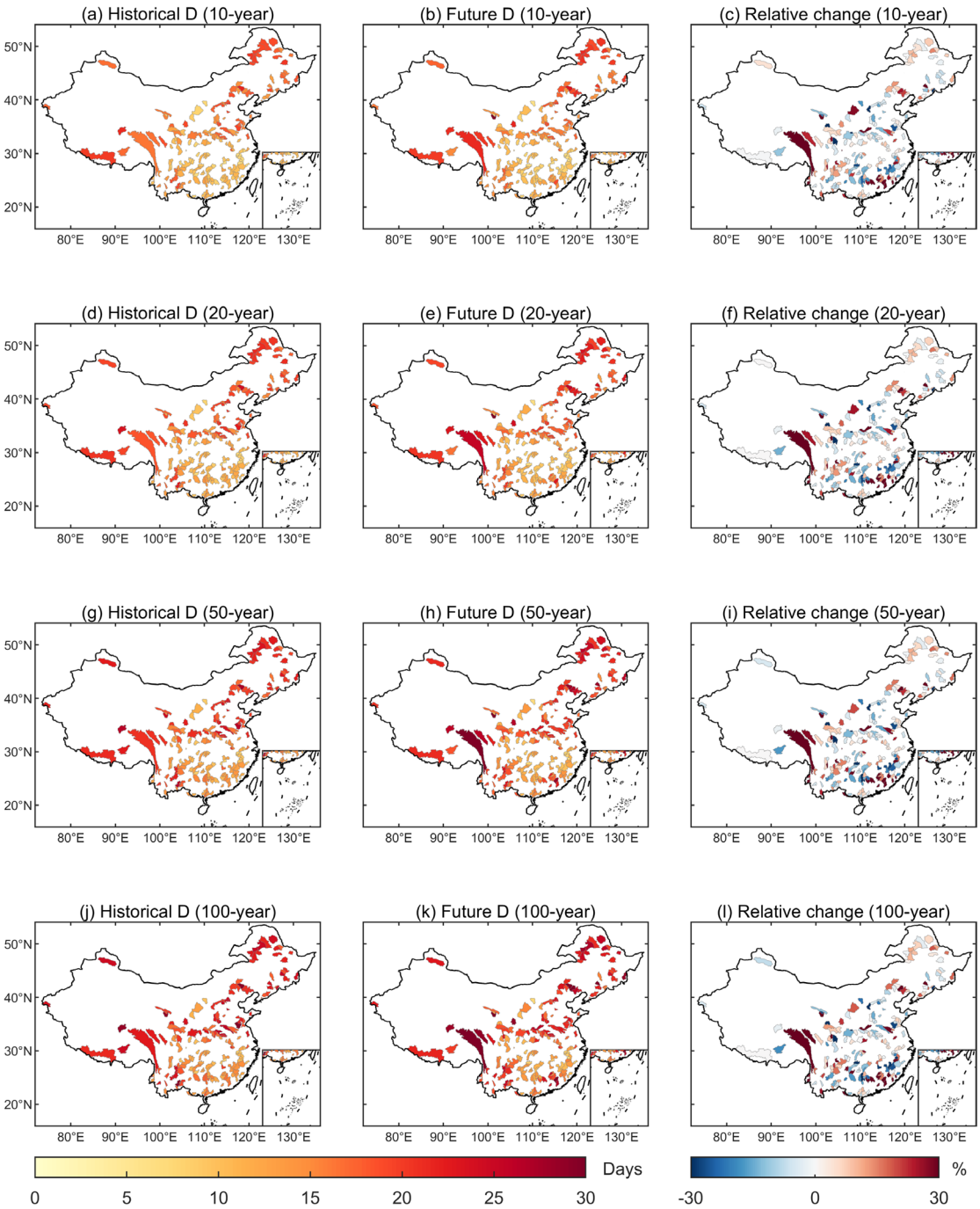

Figure S25. Flood duration under four RPs and relative change from historical to future periods. The daily streamflow series are projected by using outputs of MRI-ESM2-0 under SSP5-85.

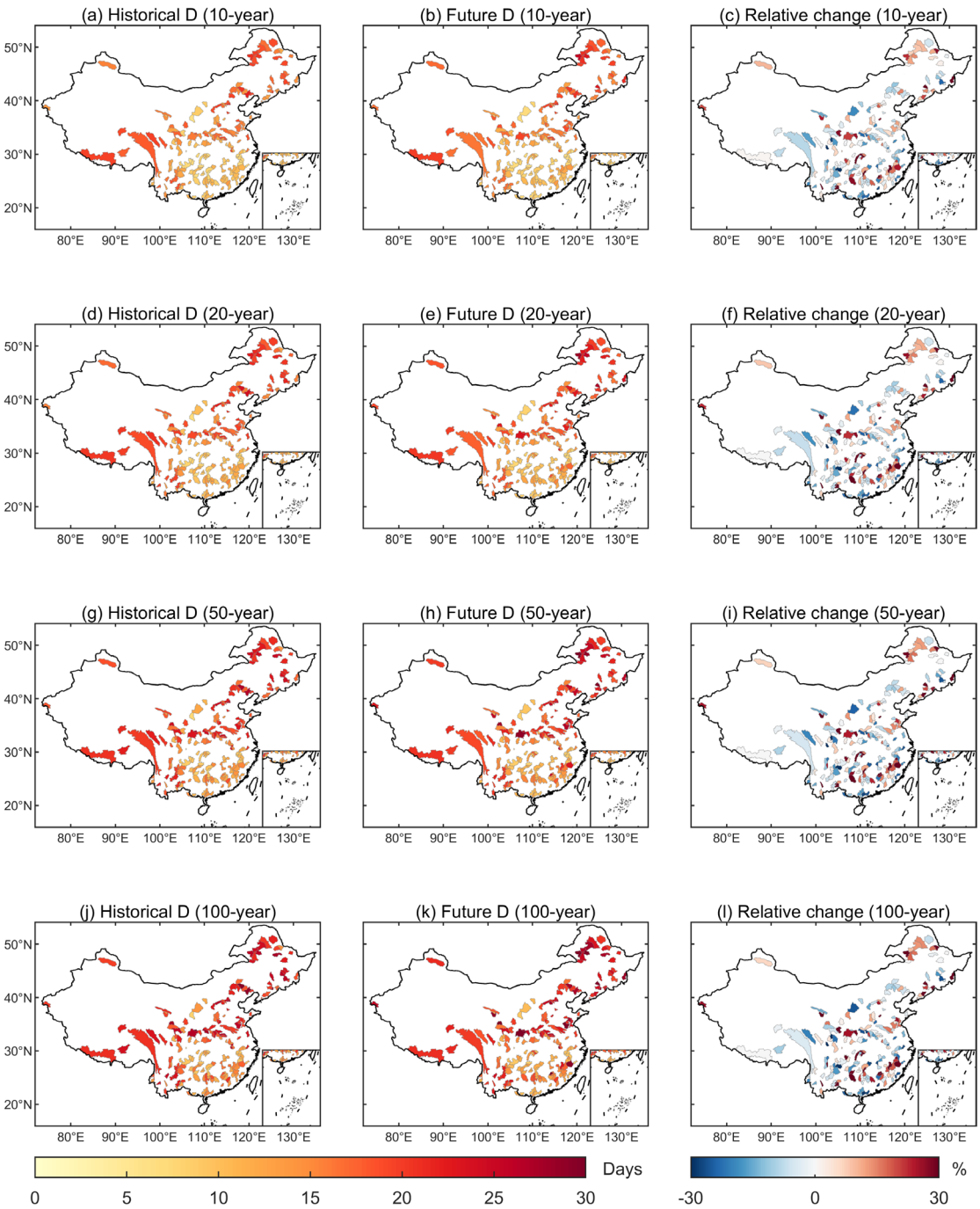

Figure S26. Flood duration under four RPs and relative change from historical to future periods. The daily streamflow series are projected by using outputs of MPI-ESM1-2-HR under SSP1-26.

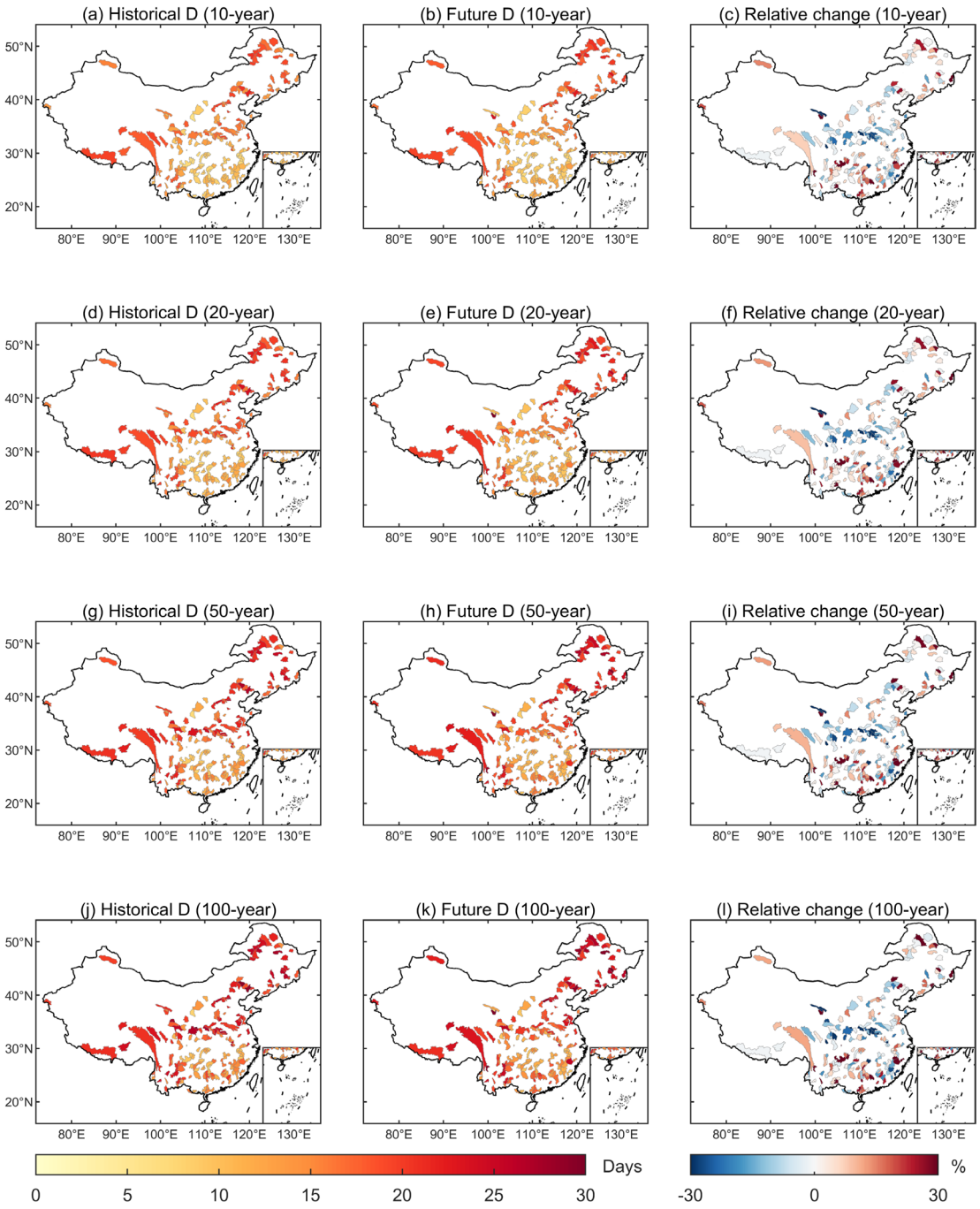

Figure S27. Flood duration under four RPs and relative change from historical to future periods. The daily streamflow series are projected by using outputs of MPI-ESM1-2-HR under SSP3-70.

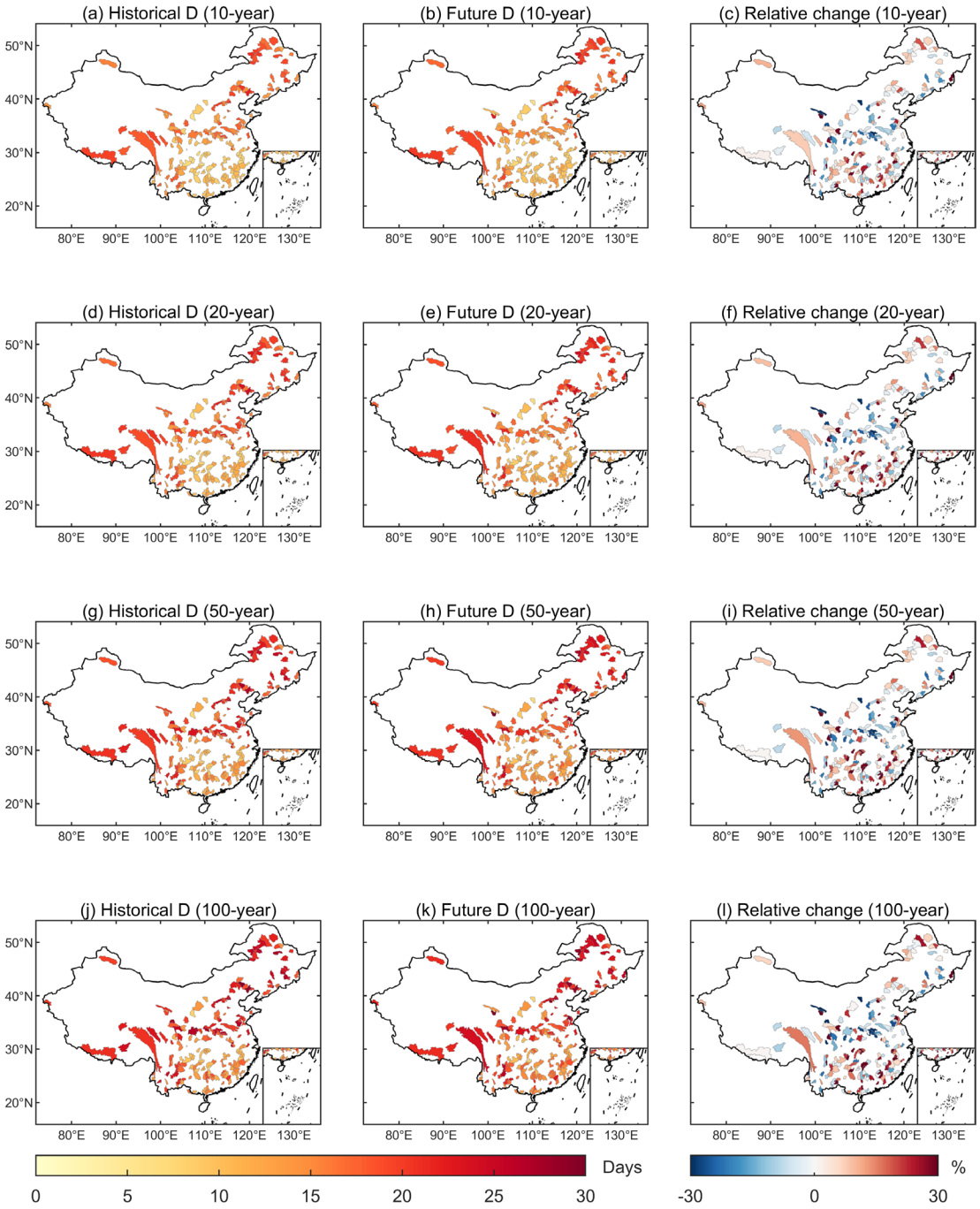

Figure S28. Flood duration under four RPs and relative change from historical to future periods. The daily streamflow series are projected by using outputs of MPI-ESM1-2-HR under SSP5-85.

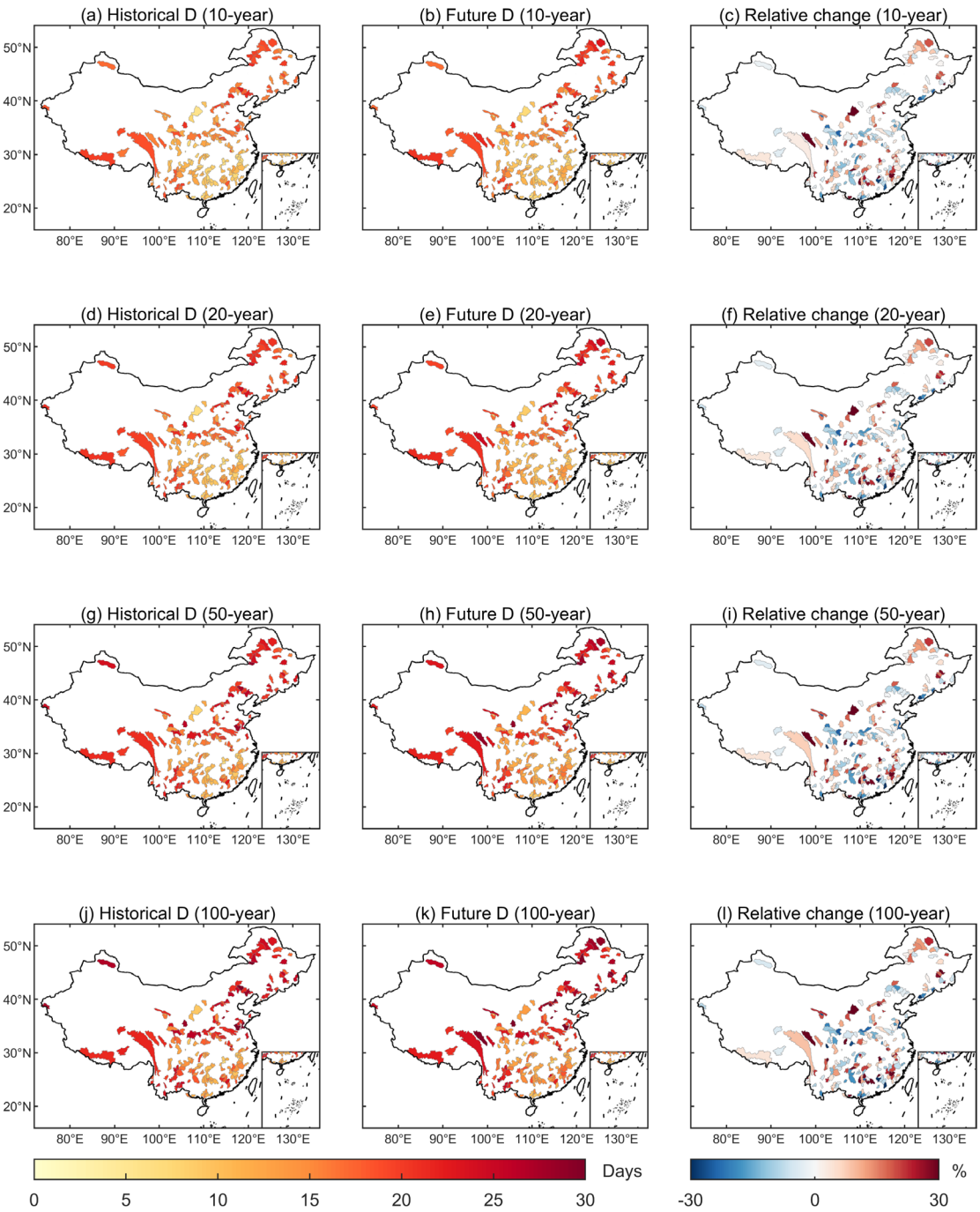

Figure S29. Flood duration under four RPs and relative change from historical to future periods. The daily streamflow series are projected by using outputs of IPSL-CM6A-LR under SSP1-26.

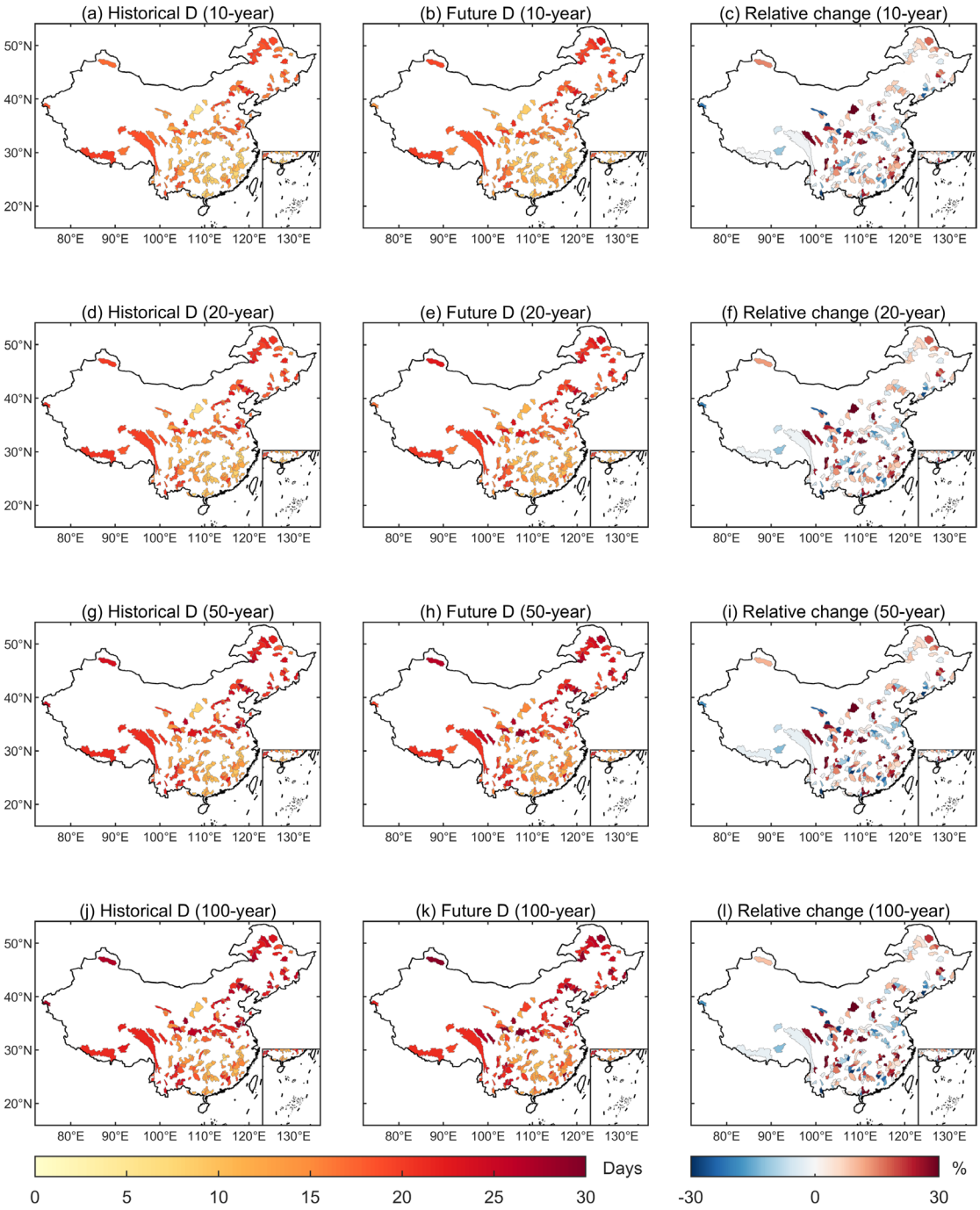

Figure S30. Flood duration under four RPs and relative change from historical to future periods. The daily streamflow series are projected by using outputs of IPSL-CM6A-LR under SSP3-70.

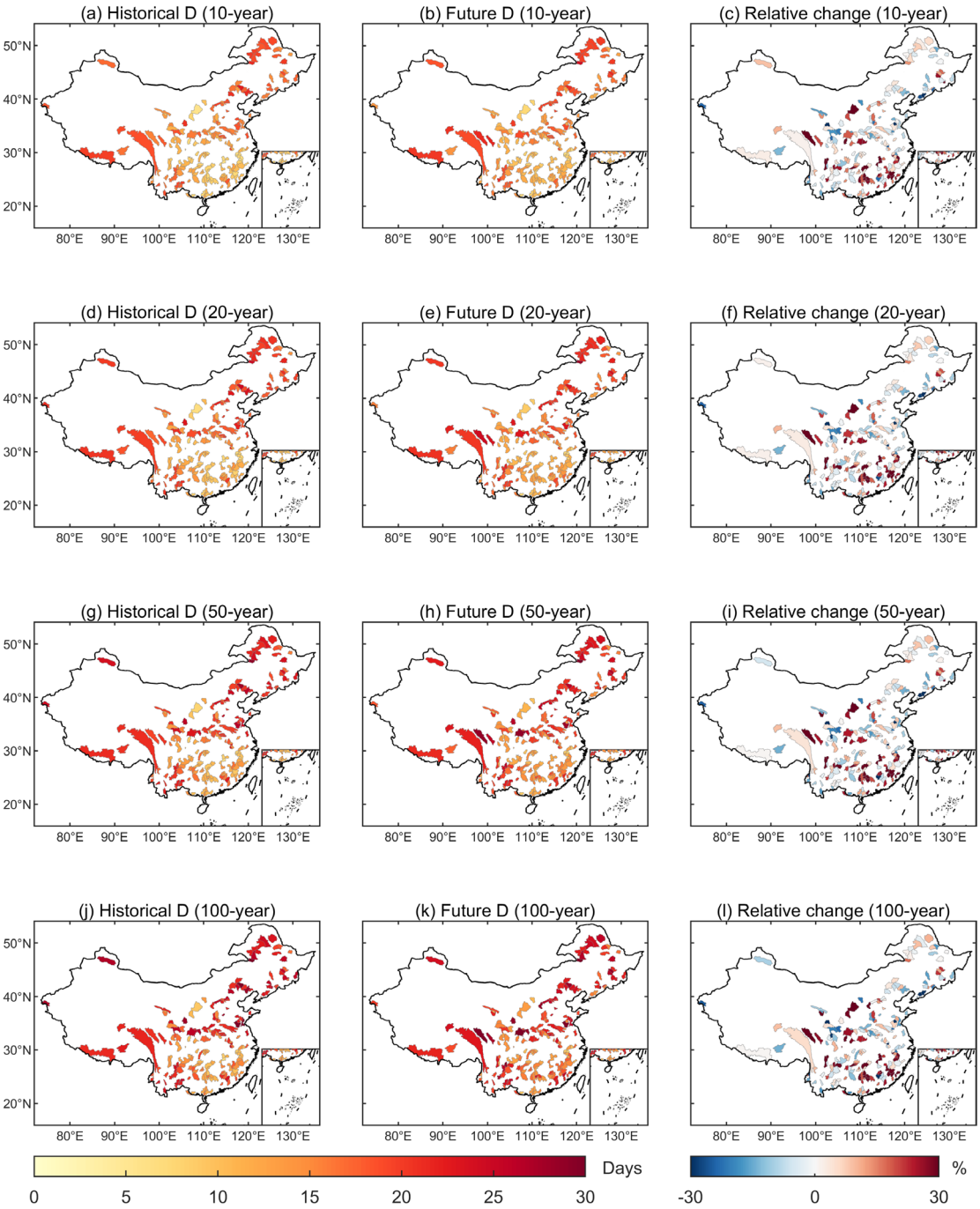

Figure S31. Flood duration under four RPs and relative change from historical to future periods. The daily streamflow series are projected by using outputs of IPSL-CM6A-LR under SSP5-85.

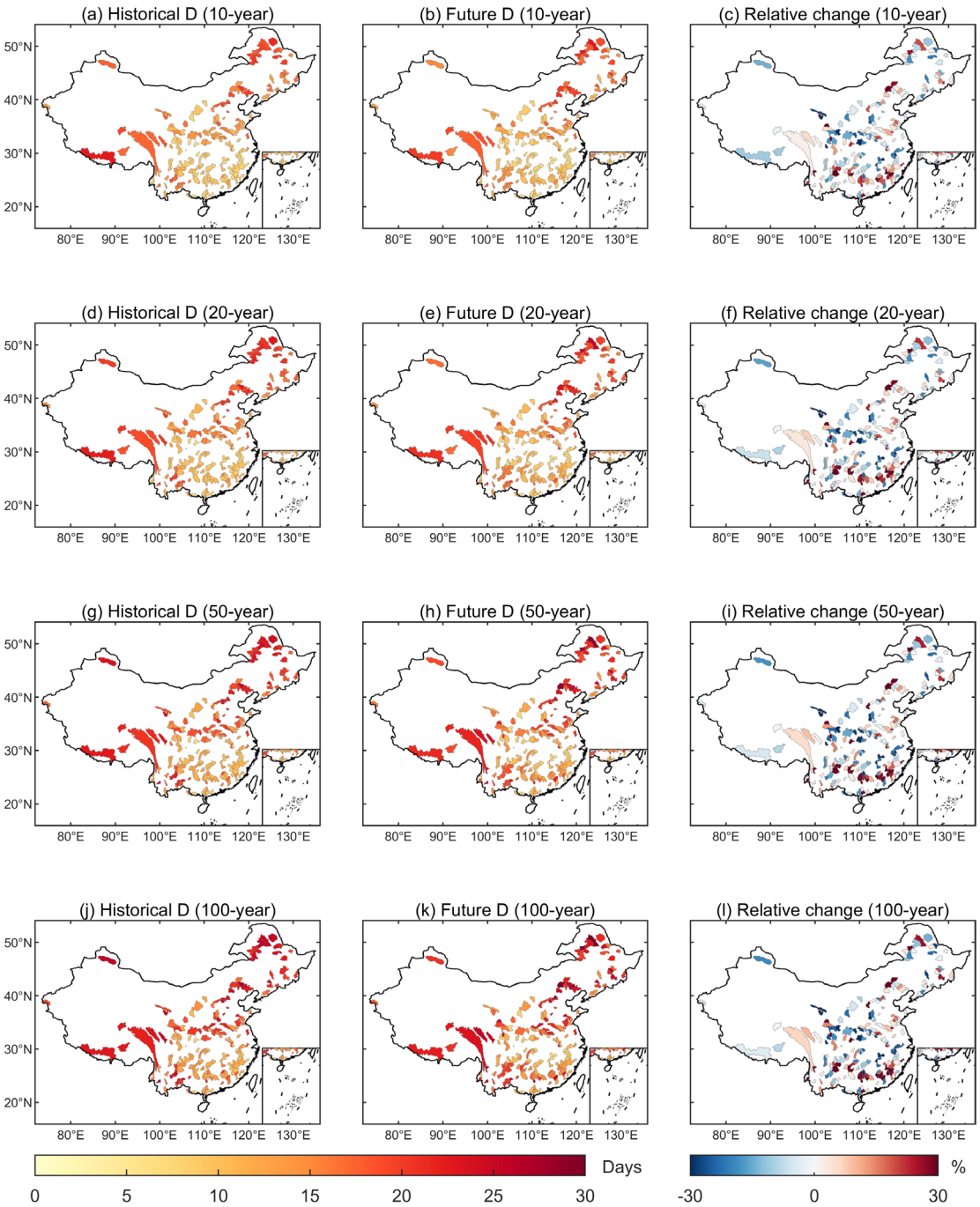

Figure S32. Flood duration under four RPs and relative change from historical to future periods. The daily streamflow series are projected by using outputs of GFDL-ESM4 under SSP1-26.

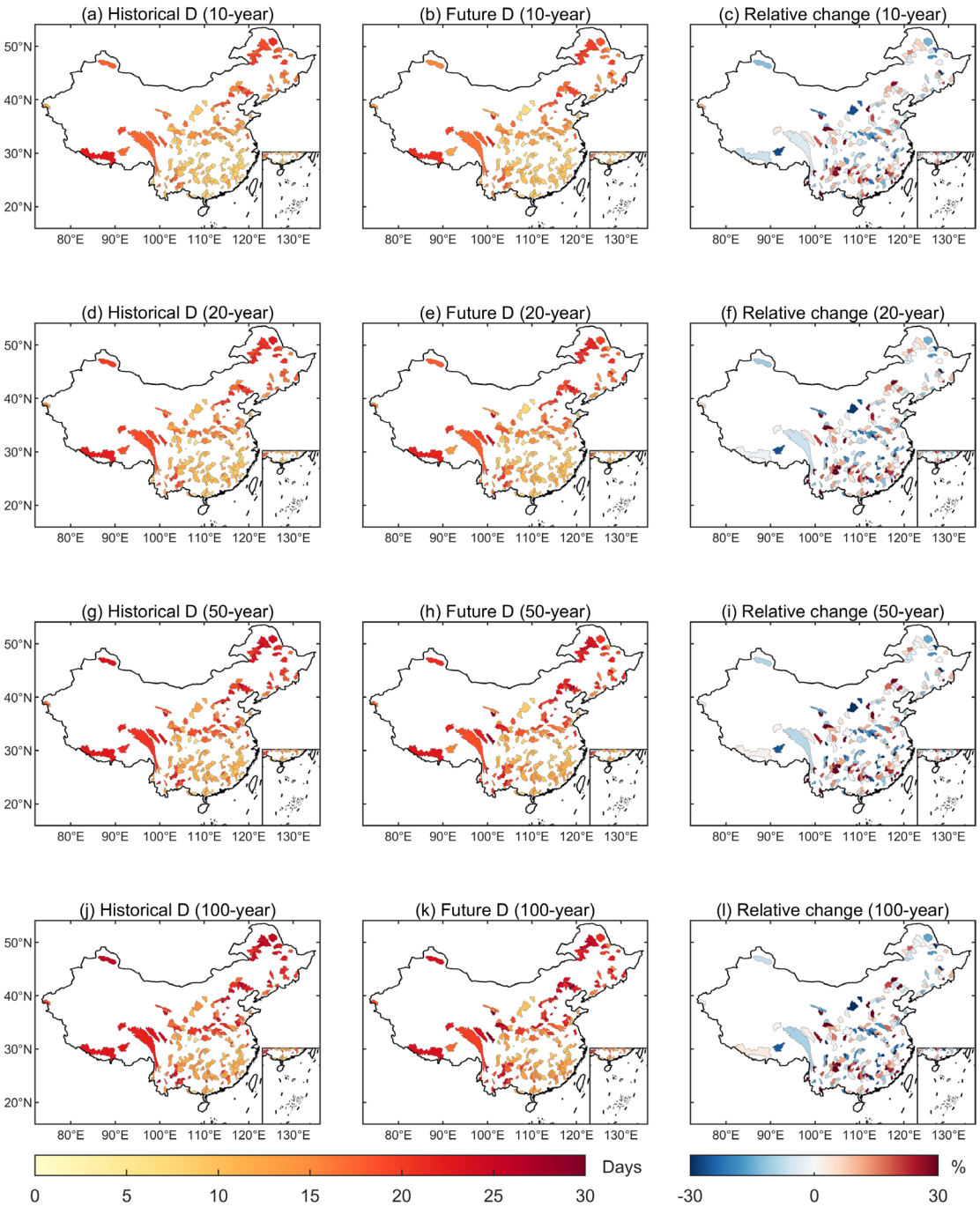

Figure S33. Flood duration under four RPs and relative change from historical to future periods. The daily streamflow series are projected by using outputs of GFDL-ESM4 under SSP3-70.

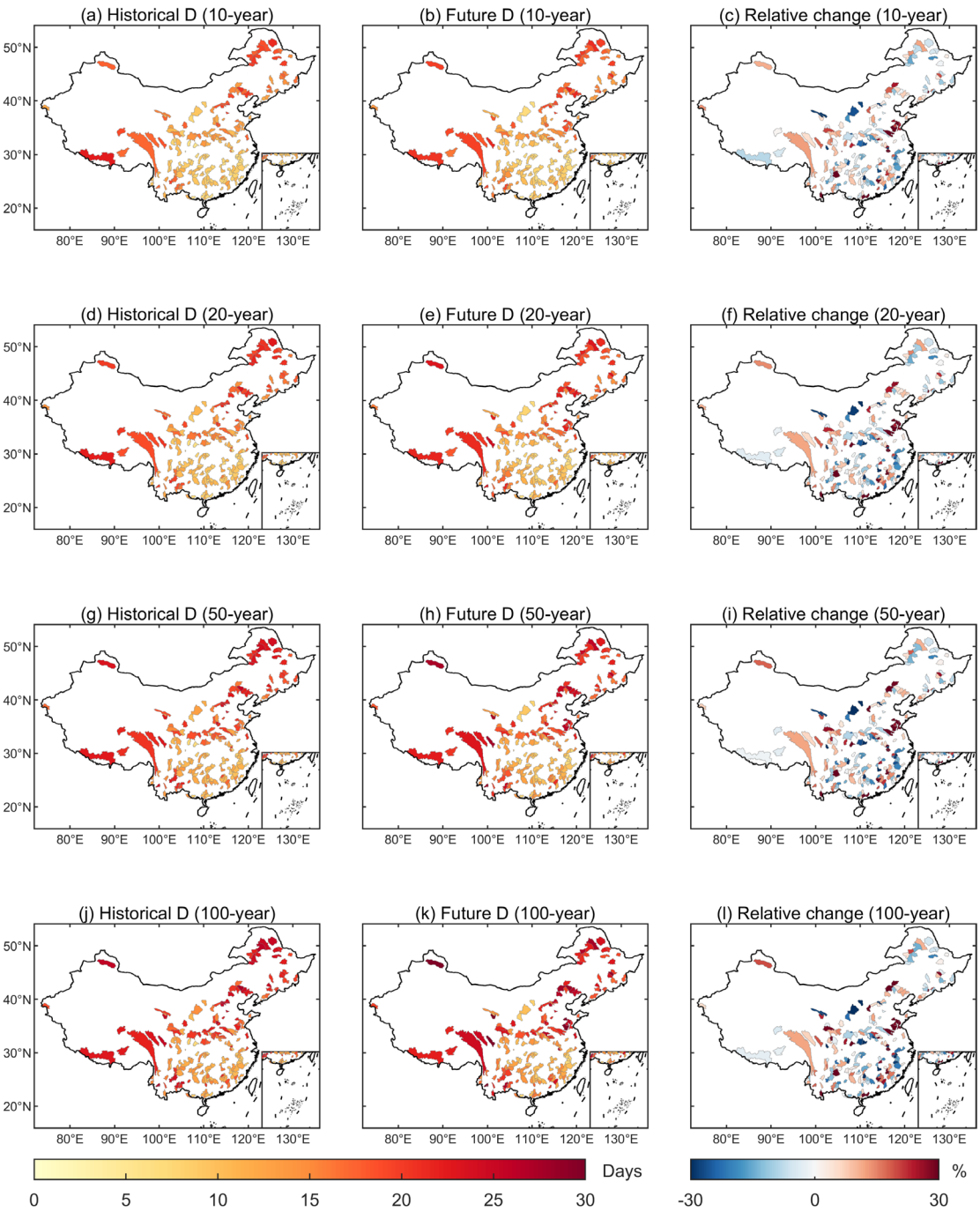

Figure S34. Flood duration under four RPs and relative change from historical to future periods. The daily streamflow series are projected by using outputs of GFDL-ESM4 under SSP5-85.

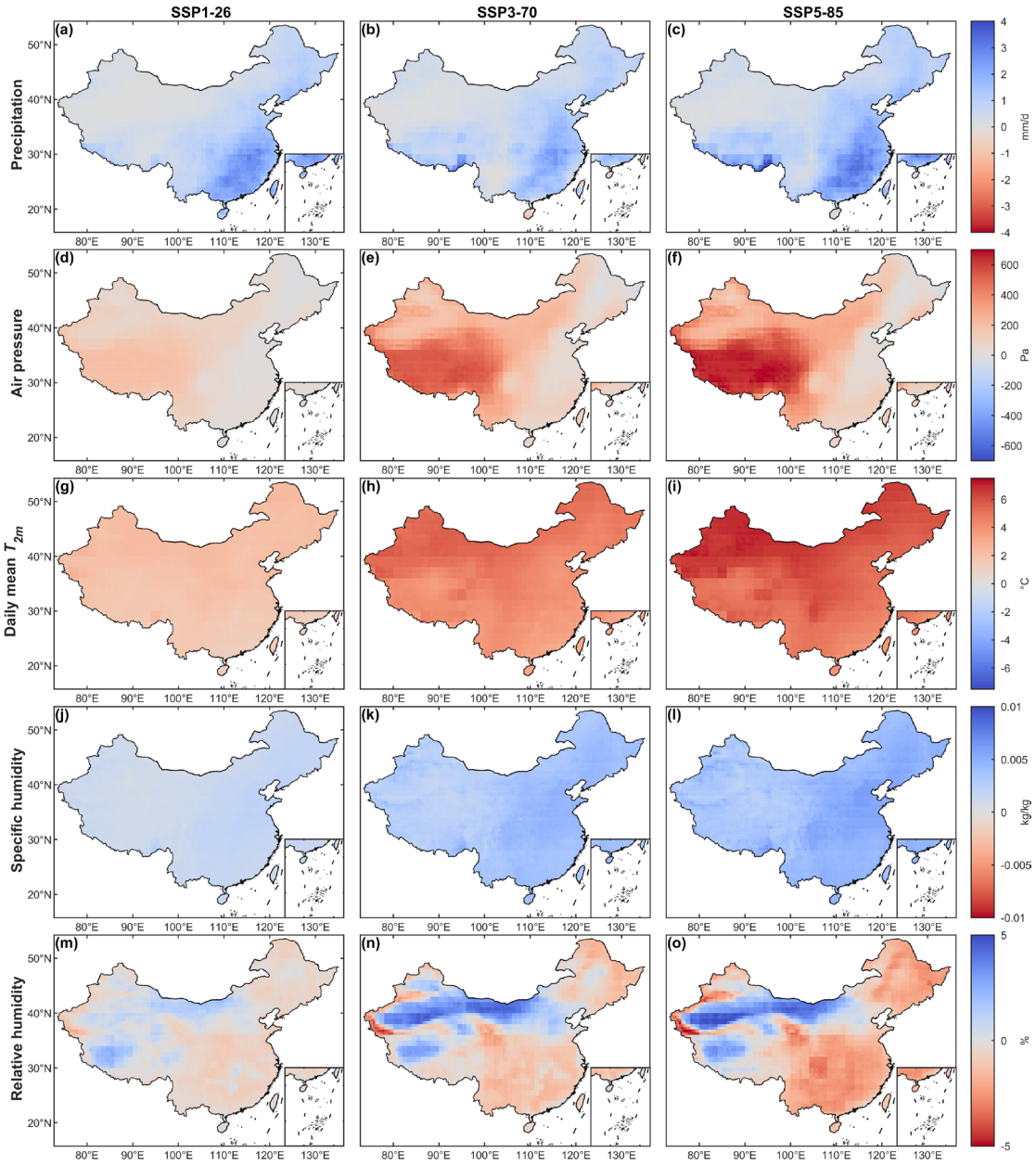

Figure S35. Changes in 90th percentile extreme values of different meteorological variables from historical period (1985-2014) to future period (2071-2100), for the three SSPs (columns). a-g, Changes of precipitation (a-c), air pressure (d-f), daily average 2m temperature (g-i), specific humidity (j-l), relative humidity (m-o).

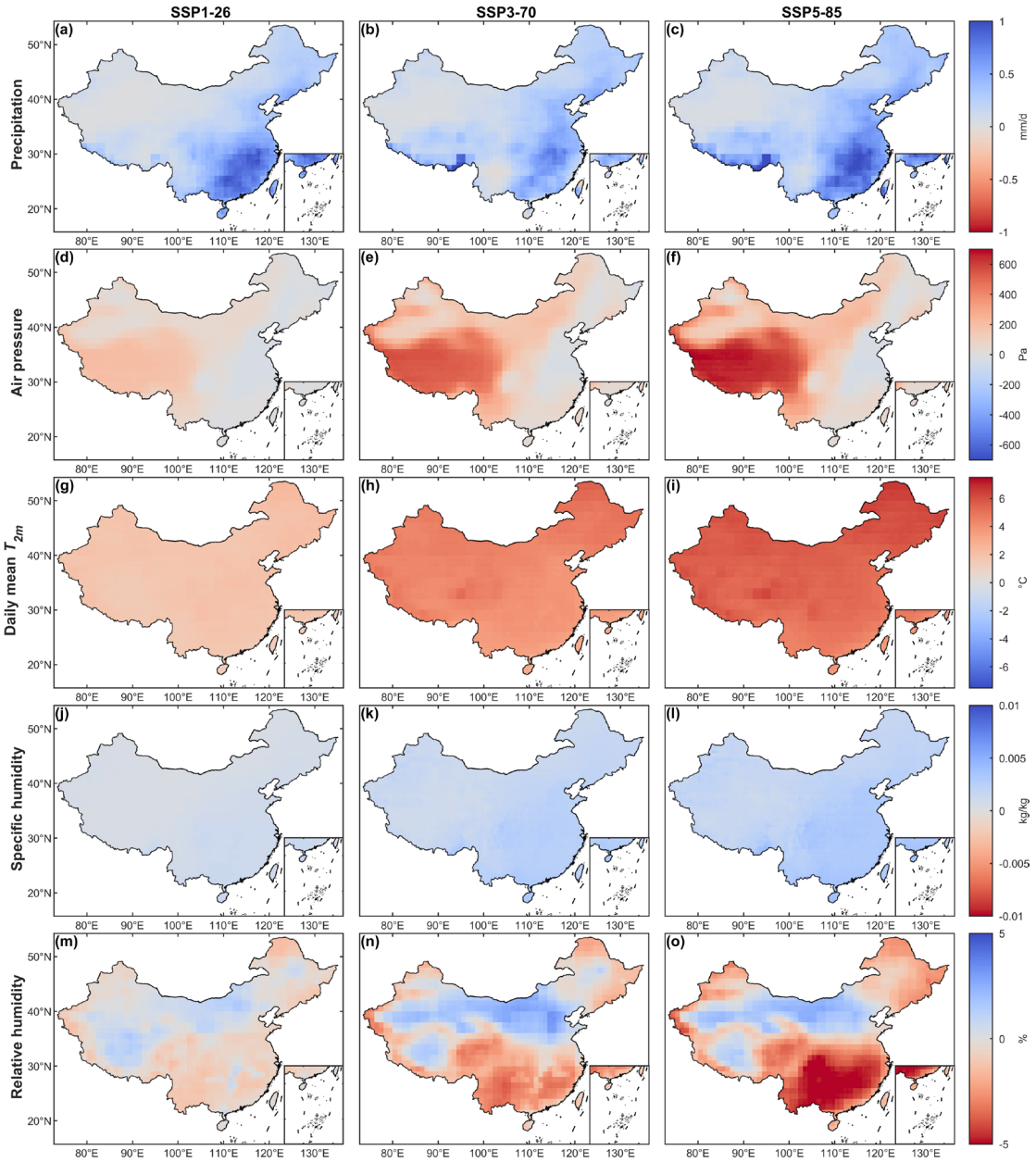

Figure S36. Changes in average values of different meteorological variables from historical period (1985-2014) to future period (2071-2100), for the three SSPs (columns). a-g, Changes of precipitation (a-c), air pressure (d-f), daily average 2m temperature (g-i), specific humidity (j-l), relative humidity (m-o).

References

Yin, J., Guo, S., Gentine, P., Sullivan, S. C., Gu, L., He, S., Chen, J., & Liu, P. (2021). Does the hook structure constrain future flood intensification under anthropogenic climate warming? *Water Resources Research*, *57*(2). https://doi.org/10.1029/2020wr028491